Millstone 2, RAI 3

DNC's response is unclear as to how likely it is that the stream of break flow will be broken-up. Based on the MPS2 audit, the NRC staff believes that a significant portion of one of the strainer arrays is located in a loop compartment beneath piping subject to breaking. Without a cover plate, it is difficult to conclude that liquid falling from the break would not fall into the containment pool above the strainer array with sufficient kinetic energy to result in air entrainment. Also, the NRC staff notes that page 7 of Attachment 1, to the December 18, 2008, DNC letter states that" ... many of the possible break locations are above a portion of the strainer and break flow in these areas would keep the portion of the strainer below the break clear of debris." It is not clear to the NRC staff why air entrainment would not occur if many of the breaks result in water falling from the break onto the strainer such that the affected portion of the strainer is continually cleared off. Also, the flow-controlling baffles inside the strainer may encourage uniform flow, but when energetic water is splashing down onto a strainer array from above, it is not clear how the baffle can limit the air entrainment to a negligible quantity. It is not clear that the strainer baffles were designed to compensate for such a non-uniform external flow. Please clarify these points.

The basis for the claim that air will escape from the strainer fins is not clear. Based on the description in the responses for MPS2, it is not clear why the 1-1/2 inch opening in the top of the strainer would perform differently than the rest of the strainer, or would not be covered with debris, just like any other strainer surface. Please clarify these points.

Regarding the Froude number discussion, the basis for the determination that air could not reach the suction pipes based on the Froude value was not clear. One particular point that was unclear concerned the assumed size of the air bubbles and whether the Froude number limit referred to was associated with vortexing or bubble ingestion. Please provide the basis or reference used for this assumption. MPS2 cites the head loss tests performed by Atomic Energy of Canada, Ltd (AECL). Some of the AECL head loss tests experienced air in the pump suction line. Please address how this impacts MPS2's evaluation of sump performance. Please address whether the Froude number was excessive for these tests (e.g., greater than 0.31). If there is direct testing evidence that could help resolve the question, please provide such documentation.

Based on the NRC staff's understanding, any air ingested by the strainer would seemingly remain trapped inside, accumulating until it was able to exit through the perforated plate or into the suction lines. Air ingestion is complex and it is unclear to the NRC staff which way the air would eventually go and how much would accumulate in the strainer before steady-state conditions are reached. The installation of a cover plate would prevent water from splashing down onto and entraining air into the strainer, removing some of complex issues associated with air ingestion.

Please address the above air ingestion concerns because excessive air ingestion can degrade operation of the pumps, which takes suction from the sump.

Response to Millstone 2, RAI 3

To minimize the likelihood for air ingestion DNC will install a cover plate during the 2R21 refueling outage. This will prevent water from splashing down onto and entraining air into the strainer.

Millstone 2, Head Loss and Vortexing, RAI 6

This RAI identified some differences in non-chemical head losses between the two test facilities. The December 18, 2008, DNC letter provided the first docketed information providing significant information on the MPS2 Rig-89 testing. The NRC staff has reviewed this and determined that the following information is needed to complete the review:

a. *Please provide information that justifies that the Rig-89 head loss test was conducted with a fibrous debris load that maximized non-chemical debris head loss.*
b. *Please provide information regarding whether the debris bed contained adequate fiber to ensure that a maximum head loss was attained without bed disturbances limiting the head loss.*

Response to Millstone 2, Head Loss and Vortexing, RAI 6, Issue 'a'

For the Millstone 2 Rig-89 chemical effects test, the thin-bed debris addition methodology was used to maximize the non-chemical debris bed head loss. The full particulate debris load was added at the start of the test, and then additions of fibrous debris were made in 1/16 inches (1.6 mm) theoretical bed thickness increments. Note that the theoretical bed thickness is defined as the uncompressed fiber volume divided by the test module surface area. The first fiber addition (1/16 inches (1.6 mm)) was made 30 minutes (enough time for debris preparation) after the addition of the particulate debris. The second fiber addition (an additional 1/16 inches (1.6 mm)) was made 30 minutes after the first addition. Previous thin bed tests conducted in Rig 33 (reduced-scale)[1] and Rig 42 (large-scale)[2] had determined a thin bed thickness of 1/8 inches.

The particulate debris load in the reduced-scale thin bed tests (Tests M2-22 and M2-27) was greater than in the Rig-89 test. In the Rig-89 test, an updated debris load was used based on Dominion Engineering Transmittal 25203-ER-07-0029 Rev 0[3]. Table 1 lists the different test debris quantities per unit test strainer surface area for Rigs 89 and 33. The particulate debris quantity was almost two times greater in Rig 33 tests than in the Rig 89 test.

At the time of Millstone 2 Rig-89 testing, it was believed that the test strainer area was 5.74 ft^2. After testing, however, it was found that the Rig-89 fin area had been miscalculated[4]. The true Rig 89 fin area was recalculated to be 5.08 ft^2. Therefore, the tested fibrous debris amount was almost 13% more than intended. The extra fibrous debris might settle on the test tank floor or attach to the debris bed loosely.

Table 1: Millstone 2 Test Debris Load Comparisons between Rigs 89 and 33

Rig	Walnut Shell [lbm/ft2]	Nukon [lbm/ft2]	Knauf [lbm/ft2]	Mineral Wool [lbm/ft2]
89	0.38	0.018	0.028	0.016
33	0.69	0.024	0.037	0.020

Since the Rig-89 test M2-C1 had only half the particulate debris amount in comparison with Rig 33 tests, the thin bed thickness of M2-C1 should not be higher than 1/8 inches. And so further fiber addition would only form a fluffy layer of fiber on top of the thin bed, which would not further increase the head loss. In order to verify this statement, all six chemical effects tests performed in Rig-89 for different strainers were compared. The peak thin bed head losses from different tests were scaled linearly based on approach velocity and quantity of particulate per unit area to match the approach velocity and particulate quantity of Millstone 2 test M2-C1, i.e., scaled head loss from Test x = (actual head loss from test x) × (M2 approach velocity / Test x approach velocity) × ((M2 particulate/area) / (test x particulate/area)). Note that the approach velocities for all other tests were higher than Millstone 2, and so scaling those head losses linearly to a lower approach velocity is conservative. The scaled head losses are plotted in Figure 1.

It can be seen that the head loss for test M2-C1 is very comparable to the other tests although M2-C1 was the only test that had 2 fiber additions of 1/16 inches theoretical bed thickness, while all other tests had 4 fiber additions. Therefore, it can be concluded that the Test M2-C1 had maximized the non-chemical head loss and further addition of fiber would not increase the head loss.

Figure 1: Comparison of Debris Head Loss for Different Stations

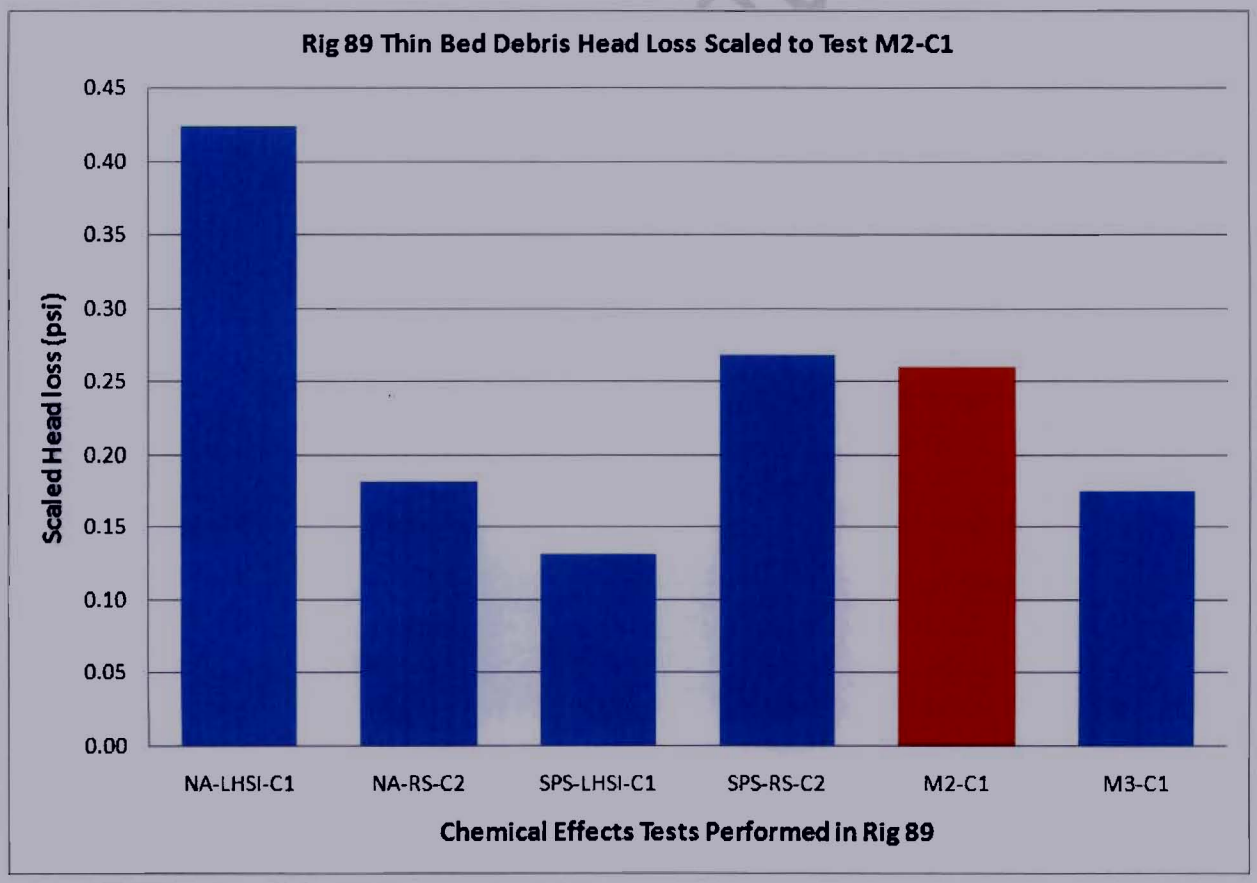

At the end of the Rig-89 test, it was found that the amount of debris attached to the fin surface was ~56%, which is quite comparable to the debris on the fin for Rig 33 tests (~58% and 66%). In Rig 33 tests it was demonstrated that the change in head loss after 1/8 inches fiber addition was insignificant. Since Rig-89 test had about the same amount of fiber on the fins with nearly half of the particulate quantity per unit area of the fins, the amount of fiber in the debris bed should be equal or more than the required quantity of fiber to form a thin bed.

Figure 2 shows the debris bed after the test. It can be seen that a uniform debris bed was formed across the whole surface of the test strainer. Figure 3 shows a portion of the debris bed removed from the strainer surface after the test.

Figure 2: Debris Bed after the Test M2-C1

Figure 3: Close up of Debris Bed after Removing from Fin

Response to Millstone 2, Head Loss and Vortexing, RAI 6, Issue 'b'

As explained above, the fibrous debris additions in the Rig-89 Millstone 2 test were sufficient to form a thin bed and to have maximized the non-chemical head loss. If more fiber were added, the extra fiber added to the test would either loosely attach to the thin-bed surface, forming a porous layer, or settle between and in front of the fins on the tank floor.

Figure 2 and Figure 3 also show that the debris bed was firm and uniform across the entire surface of the fin with no crack or hole or other degradations; also the final thickness of the bed was measured to be nearly ¼ inches, which was more than the theoretical thin bed thickness. The fully developed thin-bed thickness thus ensured debris bed structural integrity for the subsequent chemical additions.

Flow sweeps were performed at the end of the test. The changes in head loss during the flow sweeps showed no signs of hysteresis, and head loss changes were reversible. After-test debris bed examination did not find any sign of degradations, such as large holes, dislocations or fractures. Thus, the debris bed was not degraded during the test and head loss was not limited by holes in, or dislocation of, portions of the debris bed.

Millstone 2, Chemical Effects Questions

Following review of the chemical effects evaluation details in the DNC December 18, 2008, letter, the NRC staff identified that the following additional information was needed in order to determine if the testing was performed in an acceptable manner:

12. The MPS2 calcium dissolution test at a pH of 7.0 resulted in a 30-day calcium concentration of 126 mg/L. DNC's December 18, 2008, letter states that the pH 7.0 case (without tri-sodium phosphate present) was used to determine the concentration of calcium in the Rig-89 test. However, the calcium concentration used for Rig-89 testing was 40.4 mg/L. Please justify why 40.4 mg/L is a representative value in the Rig-89 testing when the dissolution testing conducted with scaled quantities of concrete resulted in a calcium concentration of 126 mg/L.

13. In Attachment 1, Table 0-2, of DNC's December 18, 2008, letter, the calcium concentration for time infinity is shown as 117 mg/L for pH 7.0. Please explain why this concentration for time infinity is appropriate, given the 30-day bench test calcium concentration at pH 7.0 was 126 mg/L.

14. DNC's testing was performed at 104°F, which is well below early post-loss-of-coolant accident pool temperatures. The solubility of calcium phosphate (hydroxyapatite) decreases as the temperature increases. Please discuss whether more calcium phosphate precipitate would have formed in the Rig-89 tests if this test would have been performed at higher temperature. If more calcium phosphate precipitate would be expected at a higher temperature, when the short-term NPSH margin is applicable, please justify why the overall Rig-89 test results provide for an adequate evaluation of chemical effects.

15. Please compare the total amount of aluminum that is predicted to be released by the AECL model with that predicted by the WCAP-16530 base model (i.e., no refinements for silicate or phosphate inhibition). Discuss any significant differences between the plant specific predictions for the two methods, including the acceptability of these differences.

Response to Millstone 2, Chemical Effects Question 12

The value of 40.4 mg/L used in the Rig 89 testing was calculated by appropriately scaling the results of the dissolution tests to match updated estimates of the Millstone 2 concrete surface area. This response will show:

1. The concrete surface area-to-volume ratio used in the bench-top dissolution tests was based on estimates of the concrete surface area that were later updated;
2. The results of the dissolution tests may be normalized to units of calcium release per unit area, which may then be used to calculate the expected calcium release and calcium concentration in Millstone 2 based on the updated concrete surface area;
3. It is appropriate to use the fit to the entire data set to determine the scaled calcium concentration rather than to scale the analysis result obtained on day 30 (126 mg/L), which is more subject to sampling and statistical errors.

The concrete surface area-to-volume (SA/V) ratio used in the bench-top dissolution tests was roughly 3 times greater than the current calculated SA/V ratio using data from ERC 25203-ER-06-0007 Rev. 3 [5] and leads to the apparent discrepancy. The dissolution tests conducted from February to March, 2008, used coupons sized to meet the SA/V ratio calculated from Rev. 1 of that document [6] and included scaled quantities of fibrous debris. Table 2 compares the SA/V ratio used in the dissolution tests to those calculated from the source references. It is important to note that, by design, there is no uncoated concrete within the Millstone 2 containment and that all values quoted are conservative estimates of bare areas exposed either by chipping and wear or by impact of the break jet [5].

Table 2: Comparison of Dissolution Test Concrete SA/V Ratio to Millstone 2 Values

Source	ERC 25203-ER-06-0007, Rev. 1 [6]	Dissolution Test	ERC 25203-ER-06-0007, Rev. 3 [5]
Date	2007/08	2008/02 – 2008/03	2008/04
Submerged Concrete	3700 ft^2 [3.44×10^6 cm^2]	1.1×3.4×0.5 cm coupons [11.98 cm^2]	400 ft^2 [3.7×10^5 cm^2]
Exposed Concrete	2600 ft^2 [2.42×10^6 cm^2]	-	925 ft^2 [8.6×10^5 cm^2]
Volume	41,000 ft^3 [1.16×10^6 L]	4 L	41,800 ft^3 [1.18×10^6 L]
SA/V Ratio (Submerged)	2.97 cm^2/L	3.0 cm^2/L	0.31 cm^2/L
SA/V Ratio (Total)	5.05 cm^2/L	-	1.04 cm^2/L

Because the concrete SA/V ratio for containment differs from that tested, the results obtained are non-representative but may be appropriately scaled. Normalization of the dissolution test data may be performed by dividing the results (in mg/L) by the SA/V ratio (3.0 cm^2/L), as indicated by the right-hand vertical axis in Figure 4. Similarly, the fit to the calcium concentration data, described below, may also be normalized to produce a calcium release equation. Thus, the 30-day calcium release per unit area of concrete can be read from the figure or calculated from the fit and used to calculate the calcium release from a known surface area of concrete.

Figure 4 also shows first-order curve fits to the data represented by Equations 1 and 2. These were determined using robust fitting procedures within TableCurve 2D† that reduce the fitting errors caused by data outliers. The constants found within Equation 1 were reported in Table 2-5 of the bench-top Test Report [7] and Table O-2 of DNC's December 18, 2008 letter. Equation 2 may be calculated from Equation 1 by dividing the initial constant by the tested surface area-to-volume ratio, 3.0 cm^2/L.

$$Ca\left[\frac{mg}{L}\right] = 117\left[\frac{mg}{L}\right](1 - \exp(-0.0072h^{-1} \cdot t)) \qquad \text{Equation 1}$$

† TableCurve 2D is produced and distributed by Systat Software Inc.

$$Ca\ Release\ \left[\frac{mg}{cm^2}\right] = 39.1\left[\frac{mg}{cm^2}\right](1 - exp(-0.0072h^{-1} \cdot t))$$

Equation 2

Figure 4: Calcium Release Data from Millstone 2 pH 7 and pH 8 Dissolution Tests without TSP at

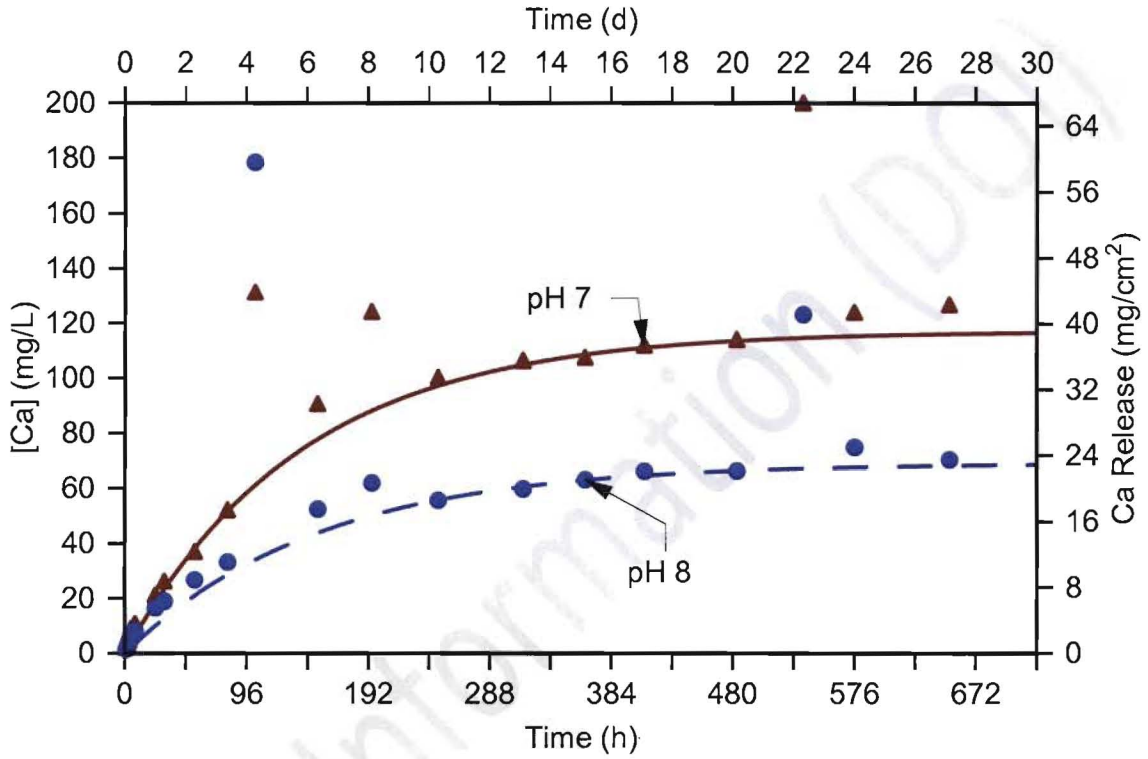

90°C

Note the lines are fits of the data sets to a first-order release equation.

It is appropriate to use the fit rather than the raw data to determine the 30-day calcium concentration, as drifts in pH, sampling errors, and statistical error associated with the analysis technique, ICP-OES (Inductively Coupled Plasma Optical Emission Spectroscopy), may alter the measured concentration.

After 30 days, the expected calcium release at pH 7 and 90°C is:

$$Ca\ Release\ \left[\frac{mg}{cm^2}\right] = 39.1\left[\frac{mg}{cm^2}\right](1 - \exp(-0.0072h^{-1} \cdot 720h)) = 38.9\left[\frac{mg}{cm^2}\right]$$

Using the total SA/V ratio from the 4th column of Table 2, 1.04 cm2/L, the expected calcium concentration is

$$Ca\ Expected\ \left[\frac{mg}{L}\right] = 38.9\left[\frac{mg}{cm^2}\right]1.04\left[\frac{cm^2}{L}\right] = 40.4\left[\frac{mg}{L}\right]$$

For comparison, the expected calcium concentration at pH 8 is 23.7 mg/L by similar analysis.

This result may be compared to the WCAP method of calculating calcium release, as described by Lane et al [8]. In utilizing this method, the calculated pH has been used; in order to maximize the release rate, the maximum pH was used to calculate the release from NuKon and Mineral Wool (around pH 8.3) and the minimum pH was used to calculate the release from concrete (around pH 8.0). By this method, the calculated calcium release from concrete is miniscule[1]; most of the calcium released comes from fibrous debris. The calcium concentration is predicted to plateau at 12.3 mg/L (Figure 5), the "saturation limit" of calcium released from NuKon at pH 8.3 and 189°F (87.2°C). Therefore, the calcium concentration obtained by scaling the AECL pH 7 dissolution test results is conservative with respect to the WCAP result.

Figure 5: Calcium release from Millstone 2 fibrous debris and concrete as calculated by the WCAP method

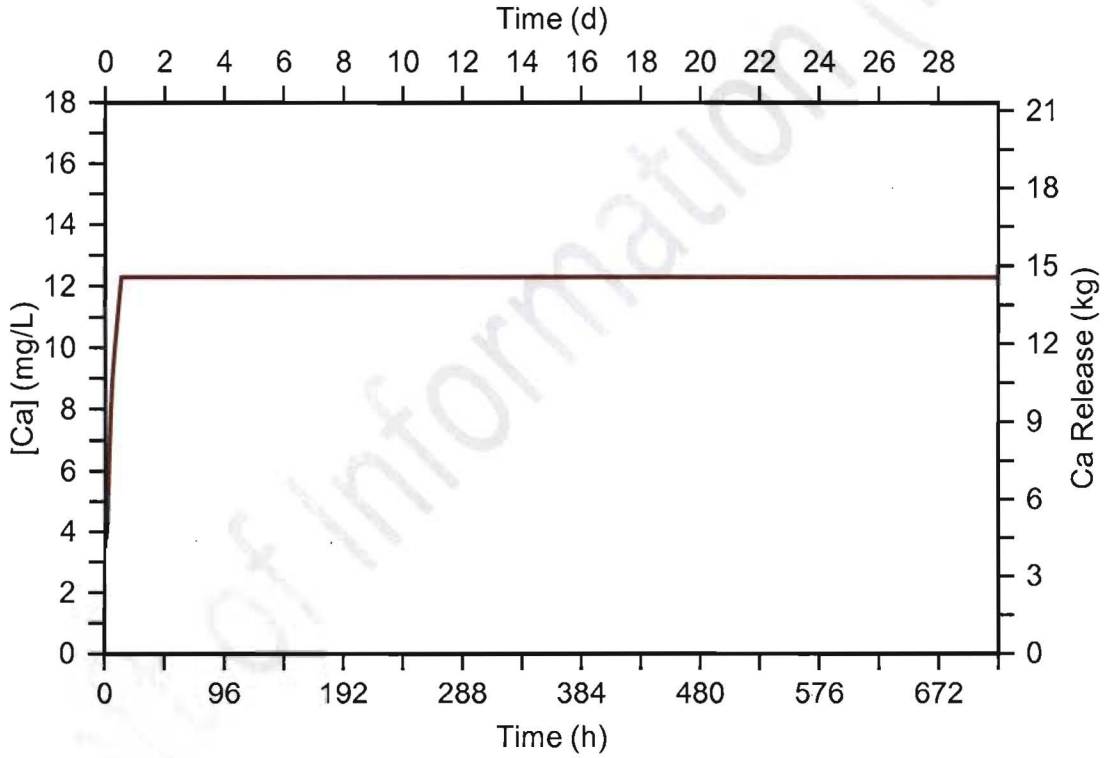

[8]

Response to Millstone 2, Chemical Effects Question 13

As with any datum, the measured calcium concentration for the day 30 sample was subject to sampling and statistical errors, with the magnitude of the statistical error alone being about ±8 mg/L. When the data are evaluated as a whole, the data fit produced by TableCurve 2D calculated a calcium concentration of 117 mg/L for time infinity; it should be noted that this value is arguably identical to 126 mg/L within the experimental error. Sources of error are further discussed below.

[1] When NuKon and Mineral Wool contributions to calcium release are neglected, the calculated calcium release from concrete using the WCAP method is less than 7 g. By contrast, when NuKon and Mineral Wool contributions are included, the calculated calcium release is nearly 15 kg.

The dissolution test data and the first-order fit to them are re-presented in Figure 6.

Figure 6: Calcium Release Data from Millstone 2 pH 7 and pH 8 Dissolution Tests (without TSP)

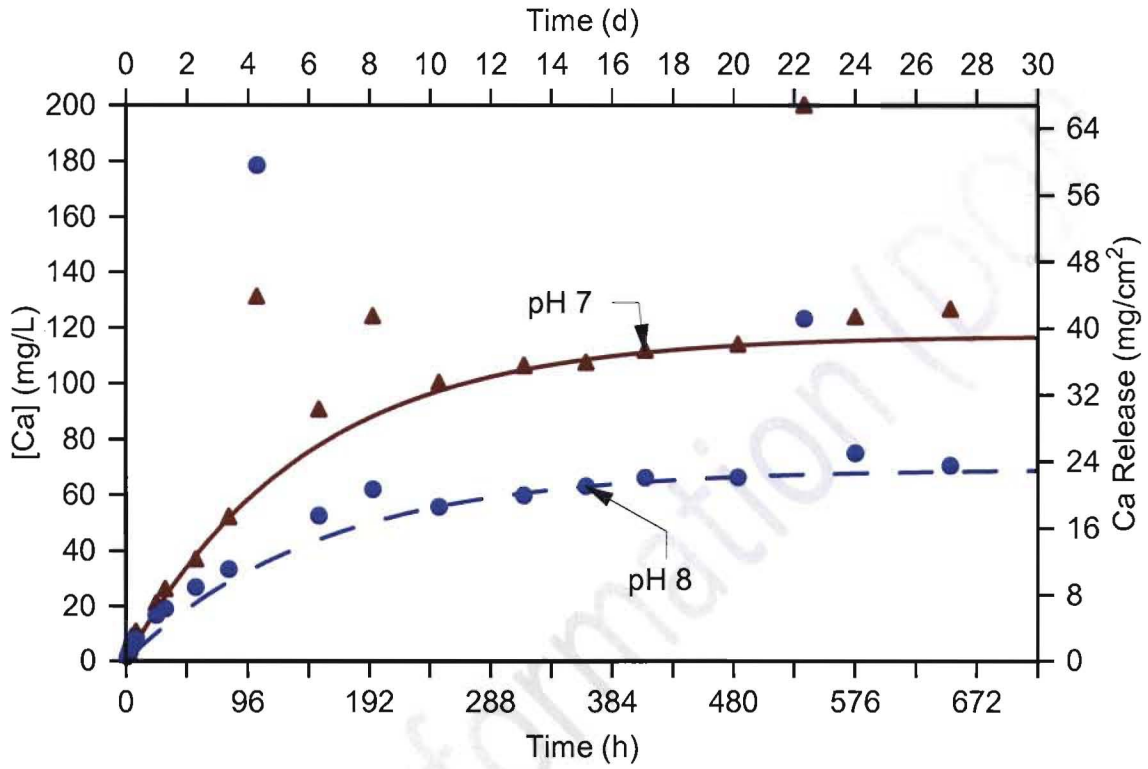

Note: the lines are fits of the data sets to a first-order release equation.

It is immediately apparent that the data contain a few outliers. It is important to consider that each datum suffers to some degree from experimental errors (e.g., position in the solution at which the tube was placed, contamination of sample vials, insufficient filtering of samples before analysis, pH drift, etc.). For example, if the sample had been taken from a location in the flask near a source of calcium (concrete or fibrous debris), the result could have been biased high. There is also uncertainty (statistical error) associated with the analysis technique, ICP-OES (Inductively Coupled Plasma Optical Emission Spectroscopy); this uncertainty was approximately ±8 mg/L for the 117 mg/L measurement. Therefore, considering all sources of error and uncertainty, there is no statistically significant difference between 117 mg/L and 126 mg/L.

Response to Millstone 2, Chemical Effects Question 14

This response will show that:

1. Literature data suggest the solubility of calcium phosphate increases above some minimum temperature around 60°C

2. A large degree of supersaturation was observed during the tests, suggesting that kinetic factors play a large role in the quantity of precipitate

With these points in mind, it is argued that the Rig 89 test results provide an adequate evaluation of chemical effects.

Calcium Phosphate Solubility

Calcium and phosphate ions can form a variety of low solubility salts in aqueous solution depending on the temperature, ions present (and therefore ionic strength), pH and the Ca/P ratio in the solution. The typical sparingly soluble calcium phosphates, which are relatively stable in aqueous systems, are hydroxyapatite, $Ca_5(PO_4)_3OH$, whitlockite, β-$Ca_3(PO_4)_2$, octacalcium phosphate, $Ca_8H_2(PO_4)_6{\cdot}5H_2O$, monetite, $CaHPO_4$, and brushite, $CaHPO_4{\cdot}2H_2O$. The solubility of these phases has been typically measured around ambient temperature; the reported results, including the solubility product constants, can differ significantly from group to group.

Of the possible calcium phosphate phases, hydroxyapatite has been found to be the least soluble in water above pH 4 and the thermodynamically most stable phase of calcium phosphate. When the solubility of calcium phosphate is the factor that limits the concentration of calcium or phosphate ions in solution, it is usually expected that hydroxyapatite is the first phase to precipitate from a solution saturated with respect to its solubility. However, experience shows that $CaHPO_4{\cdot}2H_2O$ and $Ca_8H_2(PO_4)_6{\cdot}5H_2O$ can also precipitate, particularly at ambient temperatures, and the degree of supersaturation with respect to hydroxyapatite is sufficiently high that their solubilities are also exceeded. These precipitated salts tend to transform to more stable phases such as hydroxyapatite but the process may be slow, illustrating the important role played by kinetic factors.

Sparingly soluble calcium phosphates appear to show different dissolution behavior at low and high temperatures. Below 50°C, calcium phosphate solubilities decrease with increasing temperatures. At higher temperatures, above 150°C, the limited experimental data from conductivity measurements and solubility experiments show that dissolved calcium and phosphate concentrations increase with increasing temperatures. Solubility data for calcium phosphates between 40 and 100°C, which are particularly relevant to understanding the potential for precipitation in post-LOCA (loss-of-coolant accident) sump water, are not available. However, the data indicate that there is a solubility minimum between 50 and 150°C, probably around 60°C, based on the extrapolation of experimental data shown in Figure 7.

Figure 7: Dissolved Calcium Concentration in Equilibrium with Hydroxyapatite at pH

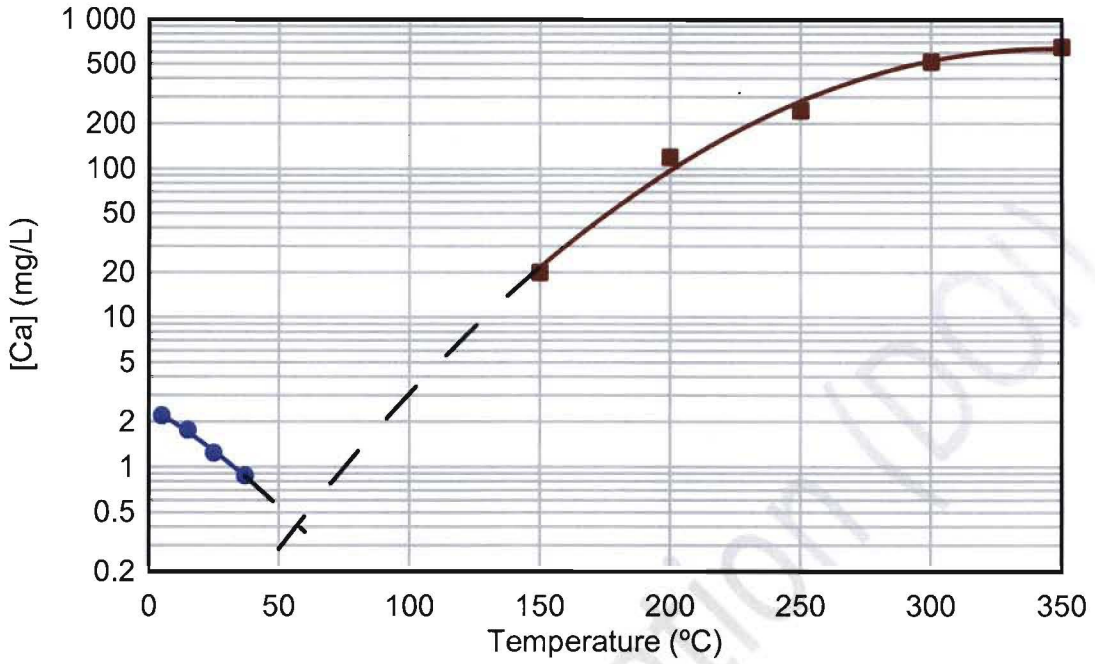

7

Note the data above 150°C were reproduced from Zhang et al [9]. The data below 50°C were calculated by extrapolation of the data of McDowell et al [10]. Solid lines represent experimental data; the dashed line is extrapolated.

For the first hour following a LOCA, when temperatures may approach 212°F (100°C) and calcium release from the various sources should not exceed 3 mg/L[2], the solubility from Figure 7 is predicted to be about 3.5 mg/L and therefore calcium phosphate is not expected to precipitate.

Kinetic Factors Observed to Affect Precipitation

The reduced-scale tests performed in Rig 89 were conducted at 40°C (104°F), pH 7 and 5000 mg/L TSP, and concentrations as high as 28.6 mg/L Ca were observed, though a quasi-equilibrium concentration was found to exist around 22.5 mg/L Ca[3]. Note that this concentration is about 28 times greater than the hydroxyapatite equilibrium concentration (Figure 7) and well above the concentration calculated for Millstone 2 by the WCAP method, 12.3 mg/L. Figure 8 shows the measured calcium concentration, which was observed to increase directly with the amount of calcium added up to the quasi-equilibrium concentration.

---

[2] Based on the WCAP method of calculating calcium release. By Equation (1), the release is calculated to be 0.28 mg/cm^2 or 0.29 mg/L.

[3] Following the 10th addition of calcium chloride to the test rig, additions ceased for 30 days, during which time the concentration of calcium was measured to be between 21.7 mg/L and 23.2 mg/L (approx. ±1.5 mg/L). This represents a quasi-equilibrium concentration, indicative of the solubility of a meta-stable precipitate, likely an amorphous calcium phosphate.

Figure 8: Calcium Concentration in Rig 89 Reduced-Scale Tests vs. Calcium Added

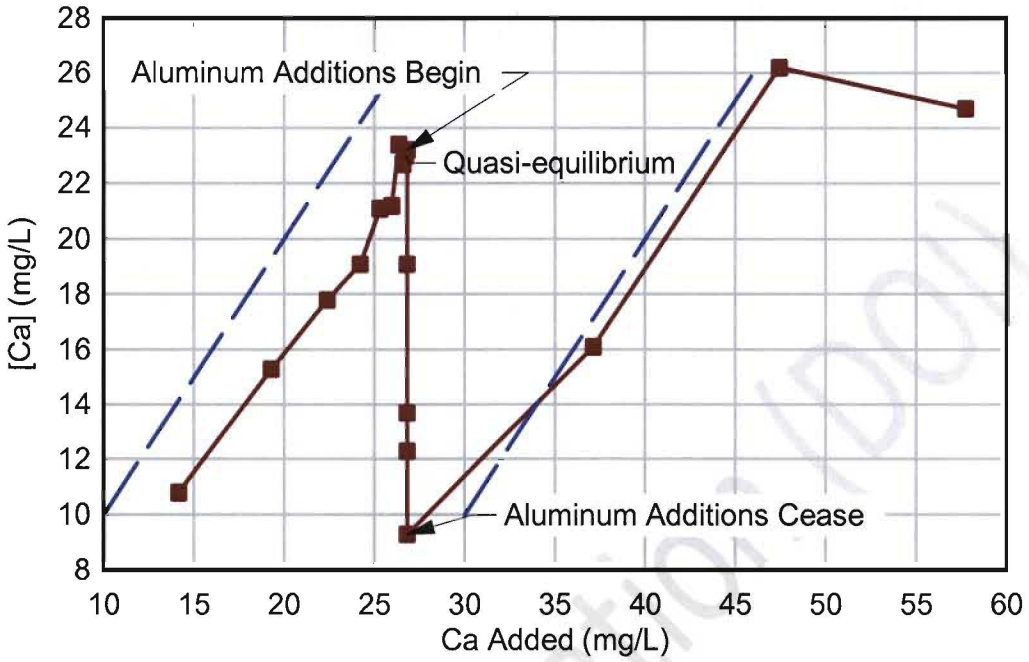

Note a quasi-equilibrium concentration around 22.5 mg/L Ca was observed during 30 days of no additions. By comparison to the dashed lines that indicate a slope = 1, it can be seen that calcium additions result in a direct increase in calcium concentration up to the quasi-equilibrium condition. Aluminum additions (one initial and seven following the 30-day hiatus) were observed to reduce calcium concentration, suggesting co-precipitation.

Summary

If Rig 89 tests were performed at higher temperature, e.g., at an early post-LOCA temperature such as 100°C or a longer-term temperature such as 65°C, the available data (Figure 7) suggest that the solubility should be greater and there should be less precipitation. Furthermore, the results of the test show that the solution is stable with respect to precipitation at concentrations greatly exceeding the calculated solubility, likely as a result of kinetic factors. Thus, the Rig 89 tests provide an adequate evaluation of chemical effects and therefore show that worst-case head loss remains within available NPSH margin.

Response to Millstone 2, Chemical Effects Question 15

The WCAP-16530 base model is an empirical model of the aluminum release rate (RR) based on the data set described by Lane et al [8], which included data from ICET 1, CR-6873, WCAP-7153A and WCAP-16530. The WCAP model is described by the Equation 3 and the results are shown in Figure 9.

$$RR\left[\frac{mg}{m^2 \cdot min}\right] = 10^{14.69039 - 4.64537\left(\frac{1000}{T[K]}\right) + 0.044554(pH_a)^2 - \frac{1.20131T(pH^a)}{1000}}$$

Equation 3

Figure 9: 3D Illustration of the WCAP Aluminum Release Model

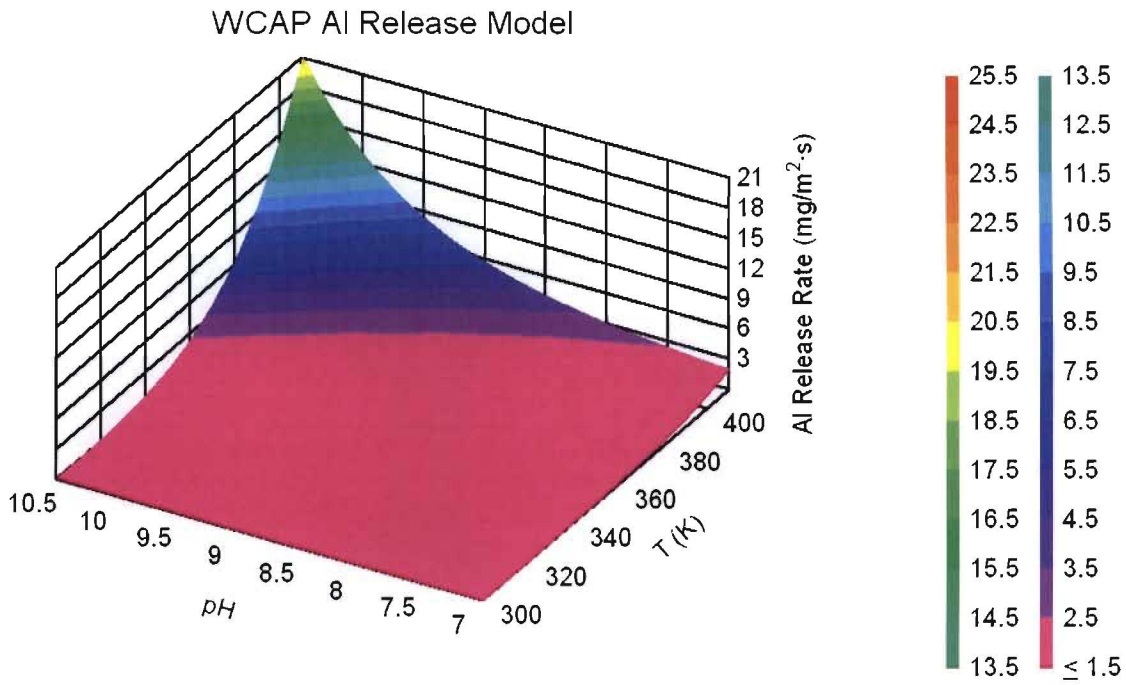

The AECL model is a semi-empirical model of the aluminum release rate, in that the equation form was developed from first principles but the parameters were fit to literature data. The release equation takes an Arrhenius form with temperature and, since the corrosion reaction involves hydroxide, the release rate is likewise related to the exponential of the pH. The data set used to fit the model was described by Guzonas and Qiu [11] and was very similar to that used for the WCAP-16530 model. The AECL model is described by Equation 4 and the results are shown in Figure 10.

$$RR\left[\frac{mg}{m^2 \cdot s}\right] = 55.2\exp\left(1.3947 \cdot pH - \frac{6301.1}{T[K]}\right)$$

Equation 4

Figure 10: 3D Illustration of the AECL Aluminum Release Model

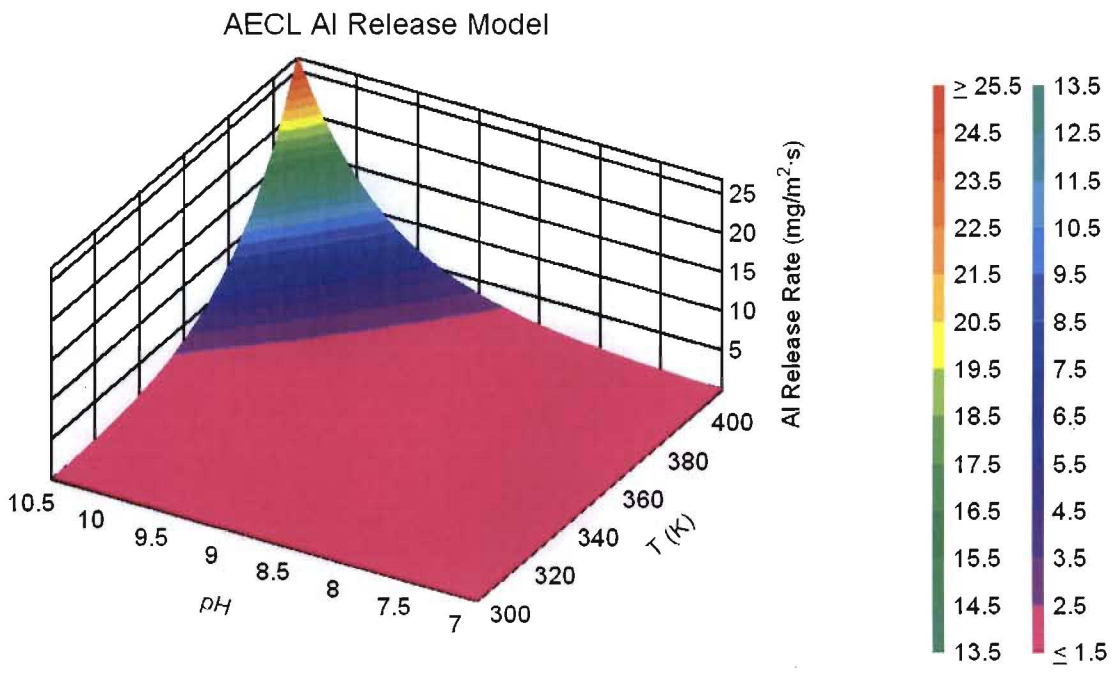

Both models ignore any time dependence of the Al release rate. As one might expect, the two models give similar predictions. Mathematical comparison of the two models shows that they differ mainly at temperatures above the normal boiling point of water. The WCAP model predicts higher release at moderate pH values (between pH 7-9.5) and lower release at high pH values, as shown in Figure 11. At more moderate temperatures, the two models predict very similar release rates. For example, ICET Test 5 [11] was conducted at 60°C at pH 8.0-8.5, and both models are observed to conservatively predict the long-term aluminum release, especially when release from sprayed aluminum with high-pH spray is included (Figure 12).

Figure 11: 3D Differential of WCAP and AECL Aluminum Release Models

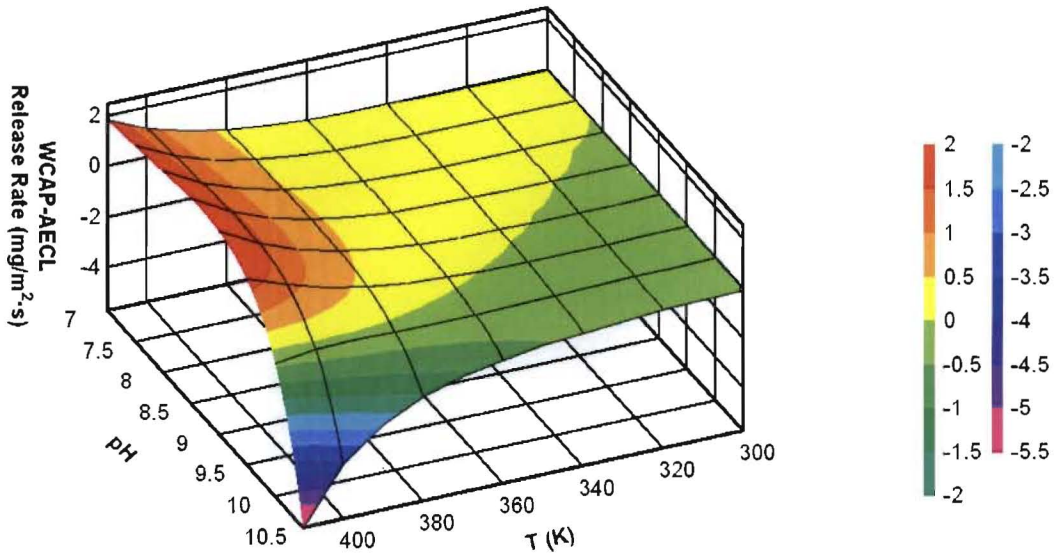

Figure 12: WCAP and AECL Aluminum Release Models' Predictions of ICET Test 5 Aluminum Concentration

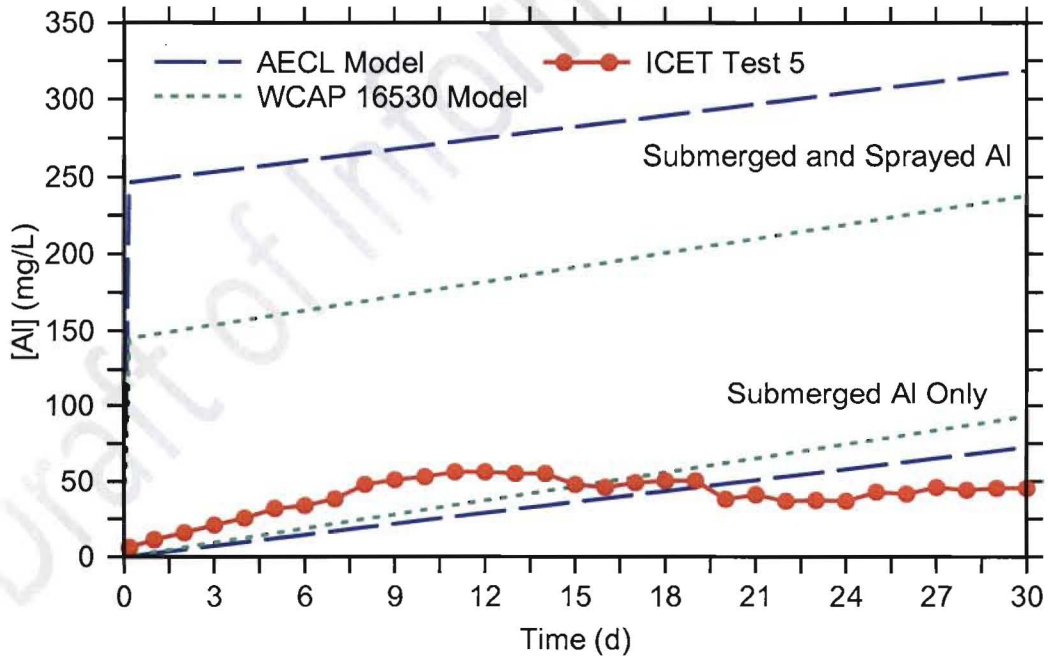

Note ICET Test 5 concentration data adapted from [11]. Spray pH, reported as < 12, was taken to be 11 for calculations.

The Millstone 2 post-LOCA sump and spray operates mainly in the range of pH 8.0-8.3, where the WCAP model predicts a greater aluminum release rate at high temperatures than the AECL model (Figure 11). For the 1876 ft^2 of sprayed and 24 ft^2 of submerged aluminum reported to be present at Millstone Unit 2 [3], the WCAP model predicts 11.9 kg Al whereas the AECL model predicts 5.8 kg Al (Figure 13). It should be noted that the scaled equivalent of 6.6 kg Al was added during the Rig 89 test[4] and that the last 5 aluminum additions (Figure 14), representing over 60% of the aluminum added, did not produce increases in head loss, suggesting a head loss plateau.

Figure 13: Comparison of AECL/WCAP Aluminum Release Models' Predictions of Submerged, Sprayed and Total (Combined) Aluminum Release for Millstone 2 Post-LOCA

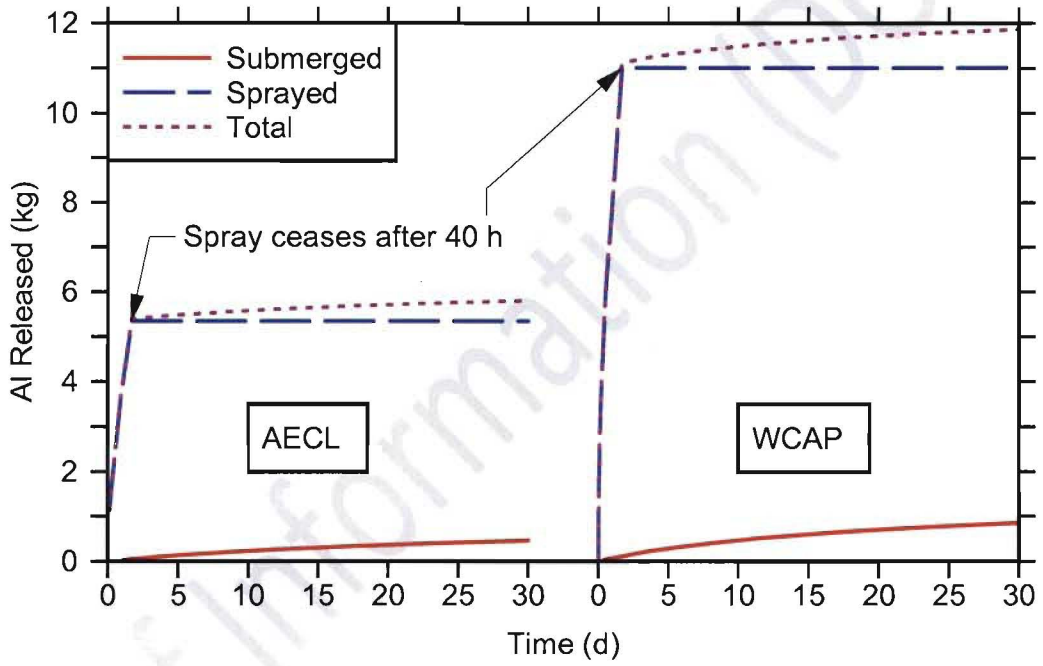

Containment

Figure 14: Rig-89 Head Loss Trace Corrected to Match the Approach Velocity of Millstone Unit

[4] Although the scaled equivalent of 6.6 kg Al was added during the test, only 6.52 kg can be said to have precipitated with certainty (i.e., the aluminum load on the strainer), as it must be conservatively assumed that the aluminum concentration is not zero but the method detection limit for ICP-OES for aluminum (0.4 mg/L).

2

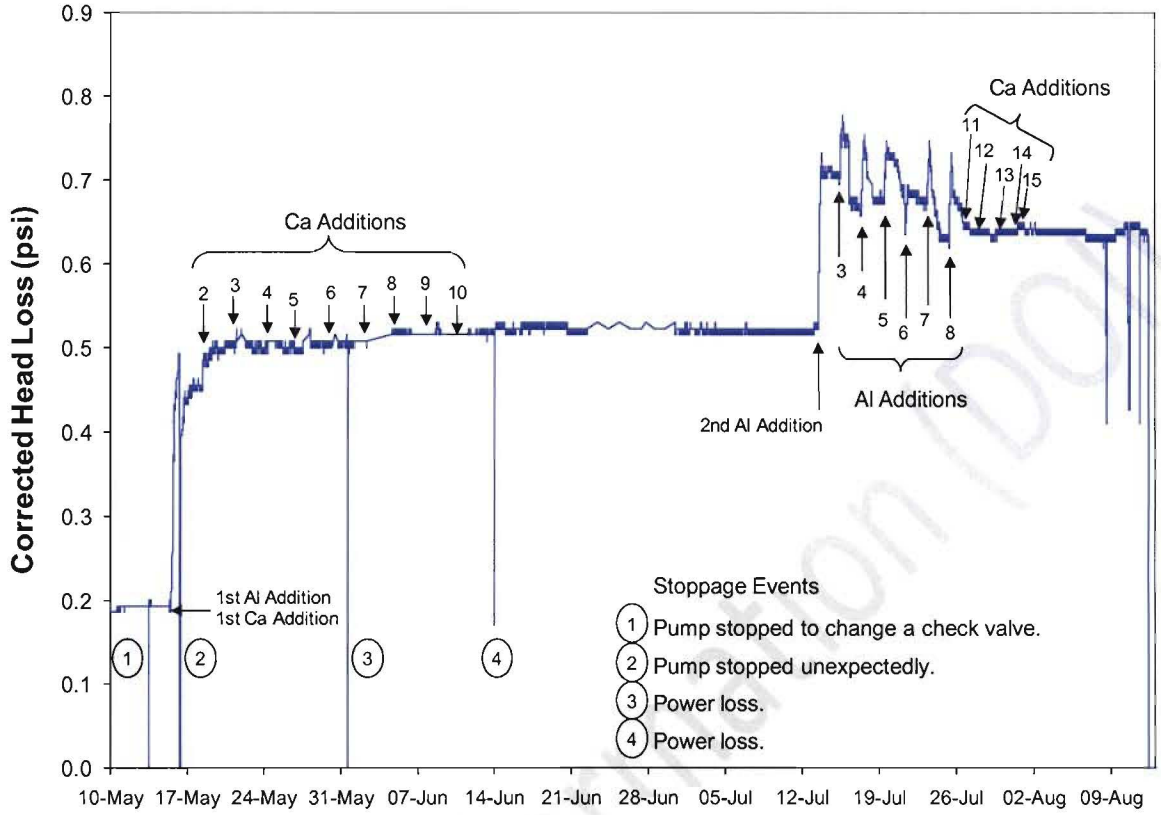

Without 30-day aluminum corrosion tests where temperatures (and pressures) of the Millstone 2 sump are simulated, it is difficult to speculate on the significance of the difference between predictions of the WCAP and AECL models. The only available data for aluminum release at pH 8 for temperatures exceeding the normal boiling point of water was reported for a 90-minute test at 265°F (129°C) by Lane et al [8]; the reported release rate of 6.6 mg/(m^2·s) was many times greater than that predicted by either model (the WCAP model predicts 2.7 mg/(m^2·s), and the AECL model predicts 1.0 mg/(m^2·s)). While this comparison may seem to highlight apparent deficiencies in both models, the deficiencies of the data set are more apparent, as it cannot be said with any certainty that the value of 6.6 mg/(m^2·s) is either accurate or repeatable. There are many variables to control in corrosion tests, and it is difficult to get consistent results; hence, Lane et al [8] could measure a release rate of 0.75 mg/(m^2·s) at pH 8 and 190°F (88°C) while others could measure lower rates at more severe conditions: Reid et al [12] measured 0.13 mg/(m^2·s) at pH 8 and 200°F (93°C), Bell et al [13] measured 0.20 mg/(m^2·s) at pH 8 and 210°F (99°C), Jain et al [14] measured 0.53 mg/(m^2·s) at pH 10 and 194°F (90°C). These values are compared to WCAP and AECL model predictions at pH 8 in Figure 15. It is clear there is a large scatter in the test data, with two data points clustered closely together and one very much higher. This may reflect differences in test methodology or conditions; AECL has found experimental uncertainties of about 30% in nominally identical tests. Both models predict release rates within the scatter of the plotted data; the AECL model better fits most of the data, but the WCAP model more closely models the average value and is the more conservative. However, the limited experimental data available do not

provide a basis for selecting one model over the other, and no significance can be ascribed to the differences in the predicted aluminum release.

Figure 15: Comparison of AECL and WCAP Aluminum Release Model Predictions and Measured Values at pH

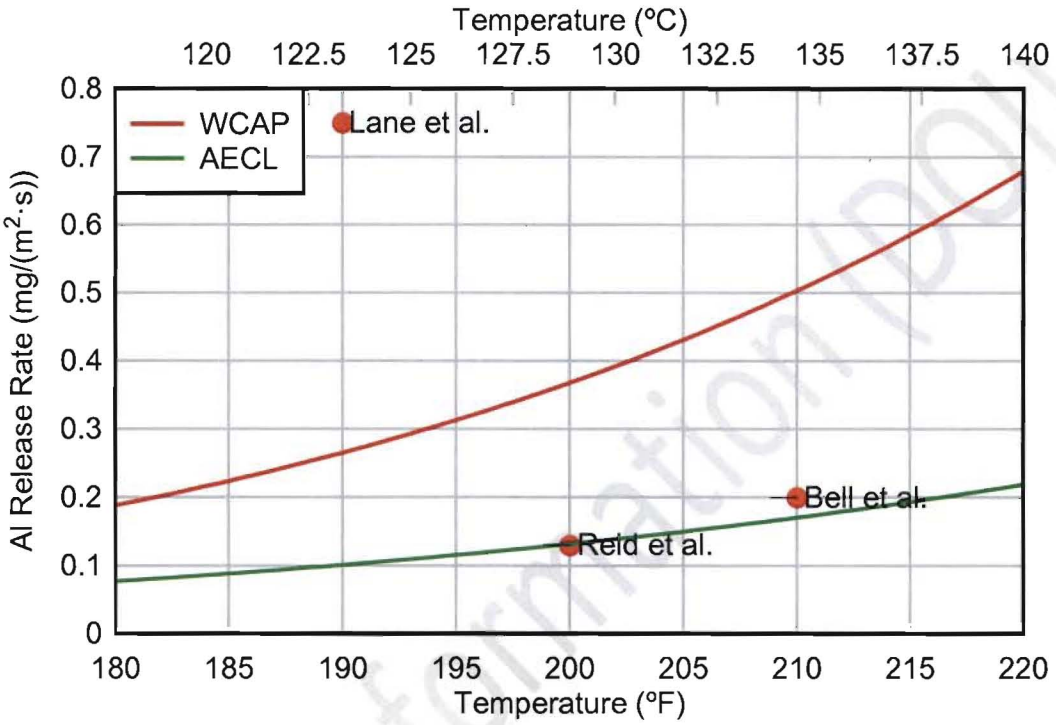

8

It should also be noted that neither model was developed to predict short-term release rates. Although short-term release rates may be higher than predicted by the models, long-term release rates are likely to be lower than predicted, as indicated by the results of ICET Test 5 (Figure 12) and other tests showing a plateau in release rates, including the classic aluminum corrosion tests described by Troutner [15, 16].

Millstone 3, Head Loss and Vortexing, RAI 6

Please provide the following additional information to document that the MPS3 strainer evaluation provides adequate assurance that it will perform as required under accident conditions:

1. *The December 18, 2008, DNC letter provides contradictory information on the amount of fibrous debris added during the test. On page 8, Attachment 2, it is stated that the limiting bed was determined to be 1/4 inch during earlier testing. Yet the same paragraph states that only two increments, containing fibrous debris to form 1/16 inch bed each, were added to the test and that no further fiber was added. Page 16 states that two 1/16 inch additions were made and implies that two further additions were made later. In addition, the graph on page 19 shows 4*

fibrous additions. Describe, in detail, the initial fibrous debris conditions of the test and the amount of any additions that were made during the test.

2. *The December 18, 2008, DNC letter states that the limiting thin bed for MPS3 is 1/4 inch as determined by previous testing. However, the head loss plot on page 19, Attachment 2, indicates that the third and fourth 1/16 inch fiber additions had little effect on head loss. Please evaluate the thin bed thickness for MPS3 in consideration of these points. Also, if the thin bed for the Rig-89 test is different from that of other tests that were used to provide Rig-89 test inputs, please provide an evaluation of how the final qualification test could have been affected by the use of such inputs. The licensee's assertion that 55% of the debris attached to the strainer for the Rig-89 test, and 72% and 84% attached to the strainer for the reduced scale test should also be considered in this evaluation.*
3. *The difference in head loss between the two test methods is about an order of magnitude. The differences in non-chemical head losses between the two types of tests were attributed to contaminants from the use of river water and to air evolution caused by non-prototypically low submergence during the reduced scale tests. It was stated that particulate and biological activity in the river water affected the head loss in the reduced scale testing. Please provide additional details on how the river water particulate and biological activity affected the head loss. Please address the following items:*
    a. *Provide an evaluation of the degree to which the particulate and biological growth from the river water affected the results of MPS3. It appears that the MPS3 tests were affected to a much greater degree than other AECL tests conducted under similar conditions. Please discuss the reason MPS3 was affected to a greater degree.*
    b. *State whether any fiber-only tests were conducted using river water. If such tests were conducted, provide the head losses and other pertinent conditions for those tests.*
    c. *Provide an evaluation of the strainer head loss resulting from the particulate that was contained in the river water. Compare the expected test result, when the particulate from the river water and the test debris particulate are present, with the result when only the test debris is considered. Provide the assumptions and the bases for the assumptions used in this evaluation.*
    d. *Provide an evaluation of whether the reduced scale testing, which was used as an input for the Rig-89 qualification testing, provided valid input due to the non-prototypical biological growth and particulate from the river water.*
4. *Please provide additional details on how the postulated air evolution affected the MPS3 head loss tests considering the following:*
    a. *Please provide an evaluation of how the air evolution phenomenon affected the MPS3 tests compared to other AECL tests conducted under similar conditions. Please provide information on why air evolution, as a factor in head losses, would only occur for AECL strainers.*
    b. *The response to RAI 4 stated that the air evolution began to affect head loss as soon as the fibrous debris was added to the test and that the head loss began to decrease as soon as fibrous debris additions were stopped. Please provide an evaluation of why the*

air evolution would begin to affect head loss as fiber was added to the test and why it would stop as soon as fibrous debris additions were stopped.

c. *Please provide an evaluation of why the evolution of air, caused by the addition of fibrous debris with air entrained in it, would result in the highest head loss when a relatively small amount of fibrous debris was added.*

5. *Figure 0-4 on page 22, Attachment 2, of the December 18, 2008, letter showed that following chemical debris additions head loss would increase, then decrease back to the pre-addition value. Please evaluate this behavior considering that it may have been caused by bed degradation. Consider whether higher head losses may have occurred had additional fibrous debris been present to provide structural support to the debris bed.*
6. *Please provide an evaluation of the potential for the lower head loss in the Rig-89 testing (versus reduced scale testing) to have been caused by agglomeration of debris, especially fibrous debris.*
7. *Please provide information that justifies that air evolution will not affect pump NPSH margins or strainer head loss in the plant. Provide the key assumptions used in the evaluation and the bases for these assumptions.*

Response to Millstone 3, Head Loss and Vortexing, RAI 6, Issue '1'

For the Millstone 3 Rig-89 chemical effects test M3-C1, four fibrous debris additions were made to the test loop to achieve a thin bed thickness of ¼ inch as determined by previous thin bed tests. The first fiber addition (1/16 in. (1.6 mm)) was made at 1504 h, May 30, 2008, after the addition of the particulate debris. The second fiber addition (an additional 1/16 in. (1.6 mm)) was made at 1750 h, May 30, 2008. The third and the fourth fiber additions (each 1/16 in.) were made at 0856 h and 1120 h, May 31, 2008, respectively. The detailed debris addition information is also indicated in the head loss vs. time curve as shown in Figure 16.

Figure 16: Debris Bed Head Loss vs. Time for Test M3-C1

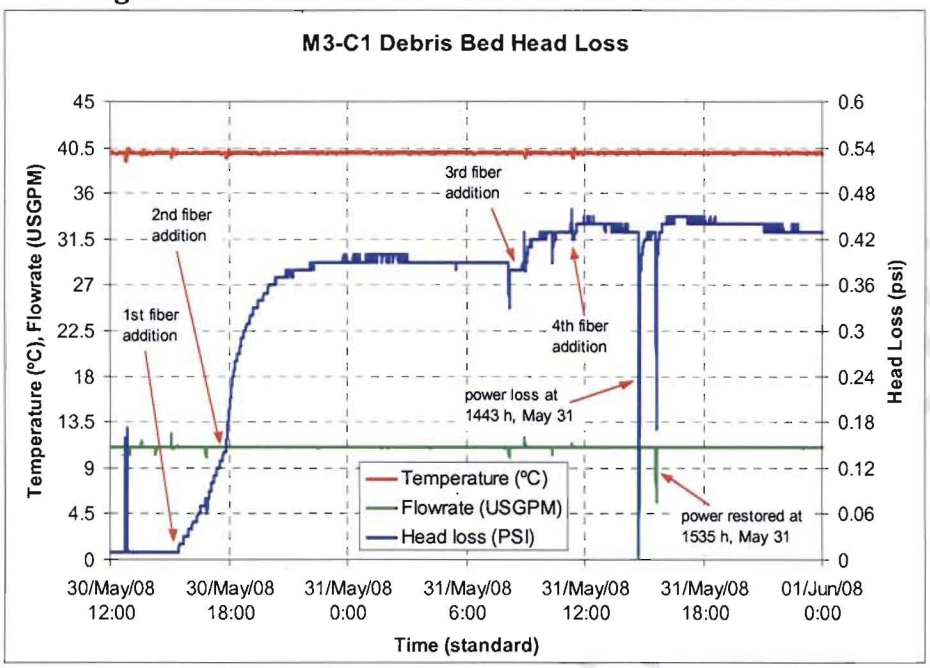

Response to Millstone 3, Head Loss and Vortexing, RAI 6, Issue '2'

As shown in Figure 16 (response to RAI 6 issue 1), the debris bed head loss increased from 0.38 psi to 0.43 psi after the third fiber addition, indicating that the thin bed thickness was at least equivalent to three additions. After the fourth fiber addition, the head loss peaked at 0.45 psi and stabilized at 0.43 psi before the first chemical addition. This indicates that the fourth addition made little difference and the thin bed could be considered to be less than ¼-inch.

The particulate debris load was 10% lower in Rig-89 test than in Rig 33 tests. Thus, the thin bed thickness would be slightly lower than that of Rig 33 tests, even though it took the same four fiber additions to form a thin bed. Also, in Rig 33, periodic floor sweeping and continuous stirring would help maintain fiber suspended and eventually attached to the debris bed. These two factors would cause a higher percentage of debris to attach to the strainer surface. The Rig-89 test head loss vs. time curve conclusively showed that a thin bed was formed by the fourth fiber addition. Extra fiber addition would not increase the head loss and would not decrease the head loss because any extra fiber lays on top of the already established thin-bed. The lower percentage of debris attached to the strainer surface as compared to that of the Rig 33 tests had no negative effects on the stabilized head loss.

Response to Millstone 3, Head Loss and Vortexing, RAI 6, Issue '3a'

Ottawa River water was used in the Rig 33 tests, while distilled water was used in the Rig-89 test. Bacteria growth and the resulting "biological effects" were observed during Rig 33 testing for Surry in 2006 May [17] and for Millstone 3 in 2006 October [18]. For the affected tests, biological activity prevented head loss from stabilizing after the second fiber addition. Slime forming was believed to be

the major mechanism for biological effects. River water particles also contributed to the higher head loss observed in those tests.

According to AECL report (AECL-1124) [19], seasonal slime formation in systems using water from the river has been a problem since 1946. Slime forming micro-organisms have the ability to grow rapidly under favorable environmental conditions. These organisms may be bacteria, fungi, algae or molds and the factors effecting their growth are temperature, pH, nutrients and concentration of electrolytes. All of these micro-organisms require a source of carbon for growth. (In the Rig 33 tests, walnut shell flour could be the ideal carbon source. The river water particulate could be another carbon source) Also reported in the AECL report 1124, a sample of the slime was sent to the National Aluminate Chemicals Company for microbiological identification. The report indicated that it consisted mainly of fungal filaments and "crystalline material". There were occasional bacteria and diatoms (Fragilaria) present.

The water level height of the Ottawa River could also affect the concentration of river particles and slime forming organisms. Higher water level resulted in higher peak head loss as shown in Figure 17.

Figure 17: Ottawa River Water Level High and Peak Millstone 3 Rig 33 Test Head Loss

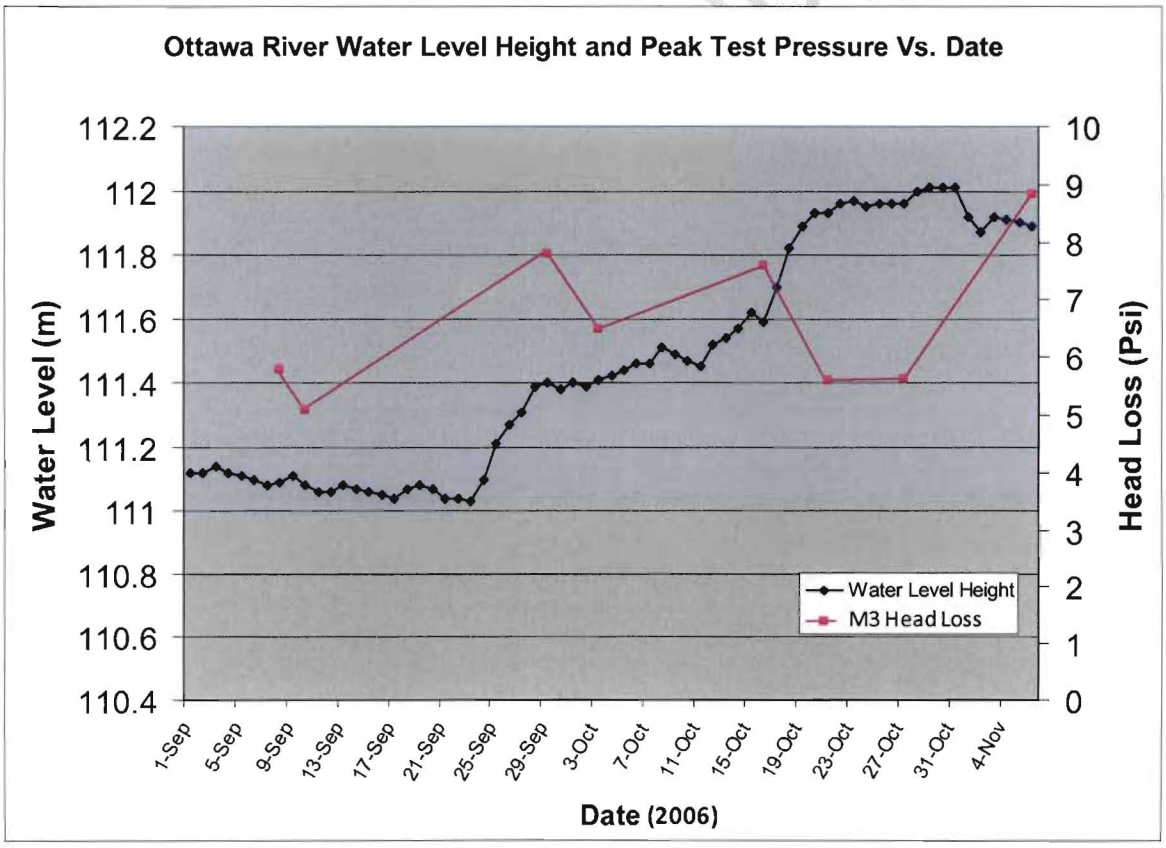

Two different water treatment methods were used in Millstone 3 Rig 33 tests to inhibit biological effects before debris addition. The water treatment method shown to effectively inhibit biological effects observed in Surry testing conducted in 2006 late-May was used for Tests M3-1 to M3-10, which were

conducted in 2006 September and October. Nitric acid (5-molar) was added to the test water to decrease the water pH to a target value of 5.5 (range of 5.1 to 5.6 pH). The test water was then heated to test temperature. Once the water temperature was stable, sodium hydroxide was added to increase the water pH to a target value of 6.8 (range of 6.5 to 7.0 pH). After debris was added, there was no further biological control.

A more aggressive water treatment was developed in 2006 November following an apparent reoccurrence of biological effects in 2006 October that affected Tests M3-6 to M3-10. This treatment, consisting of a combination of chlorine additions, heating to a higher water temperature and water filtering, was used for Tests M3-14 and M3-16. Note that filtering was instituted to reduce the quantity of particulate in the test water, not to inhibit bacterial growth. With this treatment, sufficient chlorine was added to the test water to maintain the concentration above 10 ppm during subsequent heating and filtering, as concentrations of this magnitude have been shown to prevent bacterial growth. The water heat-up procedure was changed to heat the water to a higher temperature than used previously (136°F (58°C) versus 122°F (50°C)) before cooling to the test temperature, as water temperatures approaching 140°F (60°C) are sufficient to kill many types of bacteria. Bag type filters located on the discharge side of the pump were used to reduce the quantity of particulate in the water. (This particulate consisted of small quantities of silt and rust in the service water and residual walnut shell flour from the test section and/or piping system.) Two-stage filtering was employed: a 200-µm pore size bag filter was used for the first 10 h of heat up, and a 10-µm pore size filter was used for the second 10 h. Chlorine was not added to the test tank after the first debris addition. Three samples of AECL's service water were collected during the test program and analyzed for Total Suspended Solids (TSS). The levels of TSS are shown in Table 3.

Table 3: Total Suspended Solids in Service Water

Date	Point in Test Program	TSS (mg/L)	
		Standard	Fine*
September 1, 2006	Prior to Program	0.2	n/a
October 13, 2006	Prior to Test M3-8	0.6	n/a
November 1, 2006	Prior to Test M3-14	1.2	3.0

** Note fine TSS measurements not made for samples taken prior to 2006 November 1.*

Standard TSS is measured by drawing the water sample through a 1.5-µm-pore Misa filter. The fine TSS reported herein was measured by drawing the water sample through a special 0.1-µm-pore filter.

Samples of the debris bed at the end of each test were analyzed for biological activity. This analysis is done using Biological Activity Reaction Tests (BART) for slime-forming (SLYM) and heterotrophic aerobic bacteria (HAB), followed by microbial growth on an agar media and cell counts. Analysis results are shown in Table 4. BART results are shown as positive (+) or negative (-) for microbial growth. Cell counts are shown as colony forming units per mL of water (CFU/mL).

Table 4: Biological Activity Analysis Results

Test	Sample	SLYM	HAB	CFU/ml
M3-2	#1	+	+	$4x10^6$
	#2	+	+	$3.7x10^7$
M3-16	#1	+	+	$2x10^7$
	#2	+	+	$2x10^7$

Note SLYM = slime-forming, HAB = heterotrophic aerobic, positive (+) or negative (-) for microbial growth, and CFU/ml = colony forming units per ml of water.

The analysis results show that bacteria were present in the debris bed at the end of Tests M3-2 and M3-16. Therefore, both water treatments did not entirely eliminate biological effects (the treatment method might not be effective for fungi and/or algae) It was postulated that both treatments inhibit the development of biological effects long enough to allow a test to be completed, with the aggressive treatment providing more time and/or being more effective.

Using the cell count results in Table 4, the total colony forming units in the Rig 33 test M3-16 test water would be 1 x 1014 ((2 x 107 /mL) x 5000 L), which is 5 times greater than the number of walnut shell particles (walnut shell particles: 2.0E+13). (The test tank volume is 5000 L.) Average bacterial cell is 3 to 5 µm in diameter. In the test rig, bacteria growth affecting strainer function would form a bio-film on surfaces that may be one to a few hundred microns thick. It is assumed that each colony forming unit originated from one bacterial cell. The effects of the colony forming unit on the debris bed head loss would be significant. Assuming all these colony forming units were separate spherical particles. The mass of each particle was calculated to be 3.3×10-11 g. The total mass of the slime particles would be 3.3 kg (7.3 lbm). In order to quantify the head loss influence from the slime particles, the NUREG/CR-6224 correlation was used. The calculation shows that the extra head loss increase from the slime particles could be as high as 1.2 psi.

For the river water particulate influence, an analogous comparison was performed as follows. The actual mass of suspended solids was calculated to be approximately 0.033 lb (3 mg/L × 5000 L). Assuming the increase on head loss from the river water particles were similar to that of Microtherm and the head loss influence was proportional to their mass, the head loss in Rig 33 test could be 0.06 psi higher (Head loss impact of river particulate ≈ 4.3 psi × 0.033 lb/2.39 lb ≈0.06 psi). The head loss increase due to Microtherm addition was demonstrated in Test NA-2 [20], where 2.39 lb of Microtherm was added to the test after a bed was formed. The head loss increased immediately by 4.3 psi, to a value six times greater than prior to the Microtherm addition, and the test was aborted before head loss had reached a stable value. However it is not clear that river water particulate and Microtherm have equivalent impact on debris bed head loss. In any case, 0.06 psi is an insignificant head loss impact.

The reason that the MPS3 tests were affected to a much greater degree than other Rig 33 tests was because of the test environments and the air evolution influence. Test environments include the amount of walnut shell flour and slime forming organisms in the test water. Walnut shell flour could

provide carbon to slime forming organisms as mentioned before and slime forming organisms concentrations in Ottawa River water fluctuated seasonally and were affected by the water level height. The water level height changed occasionally due to precipitation and/or discharge from the upstream hydro dam. Millstone 3 tests had the highest walnut shell flour load per unit strainer surface area among all the Dominion tests. As the debris bed head loss exceeded a threshold value, in this case, the static head of water above the fin, air evolution occurred. In the MPS3 Rig 33 tests, air evolution was the dominant factor that contributed to the higher head loss as compared to other Rig 33 tests.

In summary, several factors collectively contributed to the non-chemical head loss differences between the Rig-89 test and the Rig-33 test for Millstone Unit 3. These factors include:

- Less particulate debris in Rig-89 test than in Rig-33 test due to a refinement of post-LOCA debris load calculation (10% less),
- Distilled water was used in the Rig-89 test, while Ottawa River water was used in Rig 33 test,
- Biological growth in Rig 33 test due to the use of Ottawa River water, while no biological activity in Rig-89 test,
- Debris used in Rig-89 was autoclaved to eliminate biological growth in Rig-89. Rig 33 tests did not use autoclaved debris,
- Debris was conservatively maintained in suspension in Rig 33 in a turbulent flow outside the test section. The turbulent flow was caused by continuous stirring and return flow flushing, and,
- Large amount of air evolution in Rig 33 test while no air evolution in Rig 89 test.

Response to Millstone 3, Head Loss and Vortexing, RAI 6, Issue '3b'

No fiber-only test was performed for Millstone Unit 3, but a series of fiber-only bypass tests were performed for Millstone Unit 2, North Anna and Surry. Fiber bypass tests were conducted to determine the quantity and characteristics of fibrous debris that passes through the strainer. The full fibrous debris load was used for these tests. No particulate debris was used. The fibrous debris was "washed" to remove dirt and dust from the fibers. Fibrous debris load was added to the test tank at the start of the test within 30 minutes. For each fiber bypass test, the same test preparation was followed as its corresponding thin-bed and full debris load tests in terms of test water, heating, water treatment and debris preparation. The fiber bypass tests were usually run for several hours because the head loss stabilized very quickly. The highest observed head loss occurred in Test M2-28. The head loss stabilized at 0.1 psi. No water treatment or pre-test water filtering was used for Test M2-28. For North Anna and Surry fiber bypass tests, the head loss was negligible, for example, in Test S2-42 (Surry RS fiber bypass test), the head loss stabilized at 0.034 psi. For Test NA-19 (RS fiber bypass test) the head loss stabilized at 0.02 psi. Water treatment and pre-test water filtering were used for both North Anna and Surry fiber bypass test. The high head loss observed in Test M2-28 might verify that particulate from Ottawa River water and biological growth affected debris bed head loss.

Even though some head loss effects were observed in Test M2-28, the phenomenon was not representative because the fiber-only debris bed was too porous to catch the minute river particles and

the microscopic slime forming organisms. River water particles and slime forming organisms could cause a higher head loss if a more compact thin bed was formed.

Response to Millstone 3, Head Loss and Vortexing, RAI 6, Issue '3c'

No test results exist which directly examine the effect of the river water particulate in the absence of other variables. As briefly mentioned in response to RAI 6 Issue 3a, the river water particles could increase the head loss by 0.06 psi. The evaluation was based on the assumption that the minute river water particle would behave the same as that of the Microtherm particles on the debris bed head loss.

The calculated river water particulate mass for Test M3-16 is listed in Table 5. The mass of river particulate (0.03 lb) is insignificant and not expected to cause a measurable impact on head loss.

Table 5: Number of Particles

Test	TSS (fine) [mg/L]	Test Water Volume [L]	Total Mass of River Water Particulate [lb]
M3-16	3.0	5,000	$3.3x10^{-2}$

Response to Millstone 3, Head Loss and Vortexing, RAI 6, Issue '3d'

The inputs that were taken from the Rig 33 tests were debris preparation and addition method for thin bed forming and the specific thin bed thickness. The debris preparation and addition sequence were accepted as conservative.

There is no need to rely on any of the results of the Millstone 3 Rig 33 testing. As explained in response to Issue 2, the Rig-89 test itself demonstrated that the thin bed thickness was, indeed, ¼ inch.

Response to Millstone 3, Head Loss and Vortexing, RAI 6, Issue '4a'

Air solubility in water is proportional to the absolute pressure at the location of interest. The maximum quantity of air that could be dissolved in the water is proportional to the absolute pressure above the water surface. In strainer testing, as the debris bed head loss becomes greater than the static head of water above the fin, dissolved air will evolve from the solution. In Millstone 3 Rig 33 tests, the water submergence was set to 8 inches. The corresponding static head was 0.29 psi at the top of the submerged fin and 1.4 psi at the bottom of a 30-inch high fin. Once the debris bed head loss exceeded 0.29 psi, air evolution would start to occur along the tops of the fins and air bubbles would start to accumulate within the debris bed. When debris bed head loss exceeded 1.4 psi, air evolution would occur along the entire height of the fins. Air bubbles retained within the debris bed would restrict the flow, increasing debris head loss.

Based on a dissolved air calculation, it was found that air evolution increases significantly as the head loss across the debris bed increases. Figure 18 shows a theoretical plot of how air evolution is affected by debris head. This plot assumes that air will evolve out of solution immediately it exceeds the saturation concentration, whereas it is likely that there is some time delay and the actual air release would be less than indicated. Nevertheless, for a relatively small head loss, air evolution is very low and it starts to become more significant as head loss exceeds approximately 2 psi. The tests performed for

other Dominion plants had head losses less than 2 psi, which was not enough to cause significant air evolution.

If all the air that evolved from solution were to remain within the debris bed, with a significant head loss it would take only minutes before the debris bed was completely blocked by air. Of course, there is a constant migration of such air bubbles through the debris bed, so the bed would never get completely blocked. Under steady state conditions there is equilibrium between air evolution within the bed and air migration through the bed.

Typically, after a fiber addition the head loss increased rapidly to a much higher value, then after a while the head loss would drop and stabilize to a lower value. The air bubbles caught in the debris bed can explain this scenario. It was observed that air bubbles became attached to the fibers during the debris preparation process and were added to the test tank along with the debris, as shown in Figure 22. Shortly after a fiber addition, these air attached bubbles started to restrict the flow path, which initiated the rise in head loss and then resulted in generation of more air inside the debris bed due to low submergence. Eventually, the rate of air generation became equal to the rate of air migration, and the head loss stabilized at a lower value than the peak value. The air bubble blockage in the debris bed is believed to be the most significant factor for high head loss in Millstone 3 tests in Rig 33. Since this mechanism is strictly dependent on the water submergence and head loss, it is expected to occur for any strainer design under similar conditions.

Figure 18: Theoretical Air Evolution at a Point on the Strainer Submerged by 26 Inches

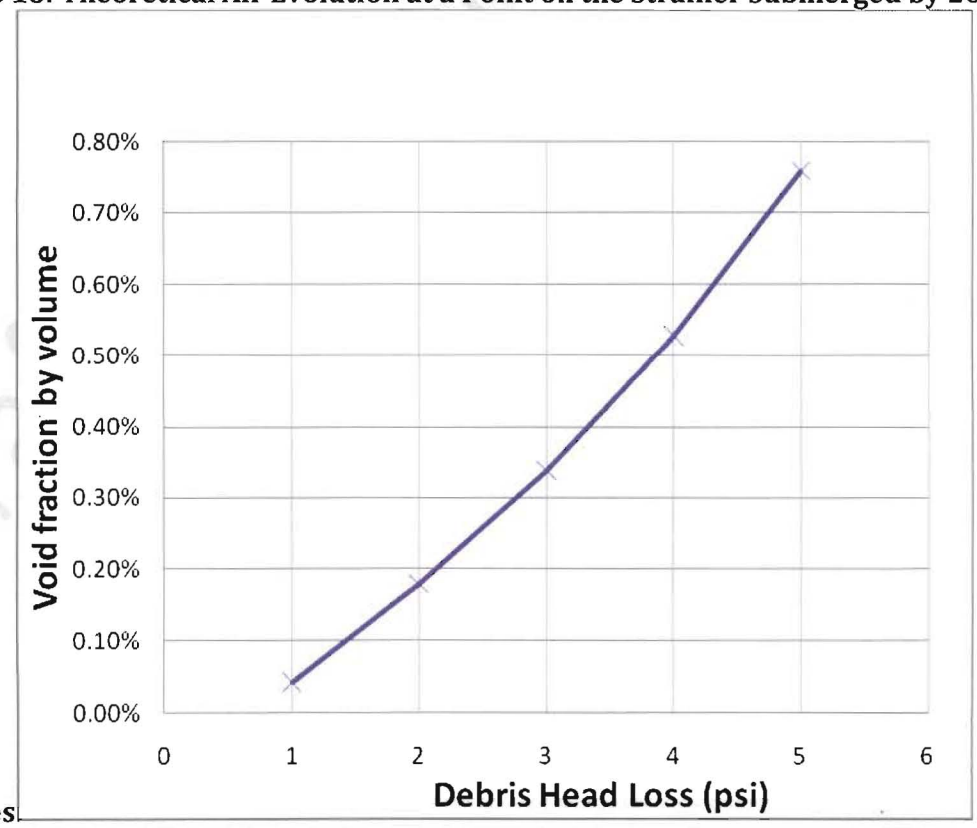

A less significant contributing factor to strainer head loss due to air evolution is accumulation of air within the strainer. Because of the test module configuration, this tended to occur in many of the Rig 33 tests.

An equation was developed in Reference [21] to calculate head loss across a strainer that is partially air-filled:

$$\Delta\rho_{void} = \Delta\rho_{full} + \frac{1}{2\rho g h} \qquad \text{Equation 5}$$

Where, $\Delta\rho_{void}$ = pressure drop across the strainer with the same uniform debris bed and flow rate when the strainer is filled with air,

$\Delta\rho_{full}$ = pressure drop across the same debris bed when the strainer is filled with water,

h = height of the air void within the strainer.

The extra pressure loss due solely to the presence of air within the strainer is quantified by the last term. This effect is due to the reduction of driving pressure for flow to pass through the upper portion of the strainer as compared to the lower portion of the strainer; thus the upper portion of the strainer loses effectiveness.

The second column from the right in Table 6 quantifies the extra head loss caused solely by air accumulation within the test strainer for all Dominion Rig 33 tests. For Millstone 3, this caused an additional 0.5 psi head loss. Moderate air accumulation was also observed during North Anna tests, which caused approximately 0.3 psi extra head loss.

The two photos below show air bubbles observed in the Millstone 3 reduced-scale test (Figure 19) and large-scale test (Figure 20).

Figure 19: Air Bubbles Observed Erupting from Fin Channels at Pump Stop in Test M3-16

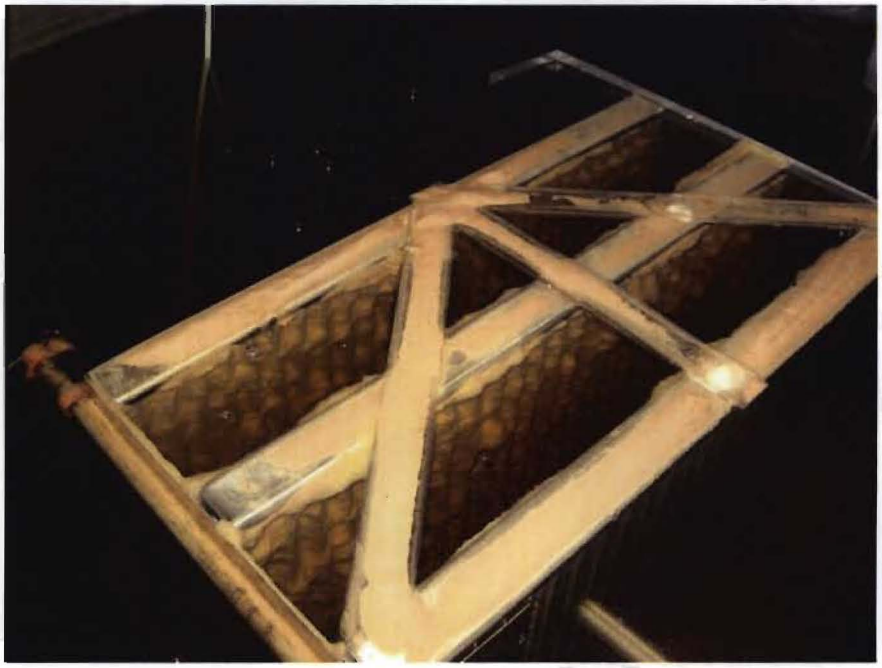

Figure 20: Air Bubbles Emerging from Discharging Header in Millstone 3 Large-Scale Test

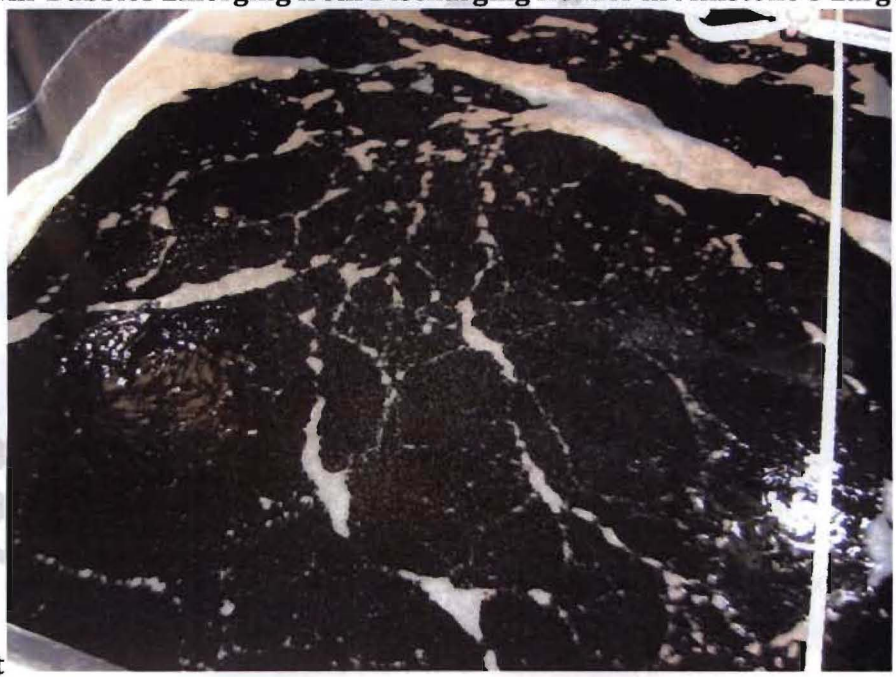

Air evolution was also observed in other Dominion strainer tests performed by AECL, but not as much. Since the debris bed head loss of these other tests was lower than that of the Millstone 3 tests, less air would be generated within the debris bed.

Similar air evolution would occur for any strainer under conditions similar to the Millstone 3 tested conditions.

Table 6: Air Evolution in Rig 33 Tests

Test	Strainer Submergence & Fin Height [inches]	Static Head Top~Bottom of Fins [psi]	Peak Debris Bed Head Loss [psi]	Head Loss Caused by Air inside Strainer [psi]	Significant Air Evolution?
NAPS LHSI NA-15	7 / 20	0.25~0.97	1.4	0.36	Minor
NA-16	7 / 20	0.25~0.97	1.3	0.36	Minor
NAPS RS NA-10	27 / 15	0.97~1.5	2.1	0.27	Minor
NA-14	27 / 15	0.97~1.5	1.4	0.27	Minor
Surry LHSI S2-33	7 / 20	0.25~0.97	0.53	0.06	No
S2-35	7 / 20	0.25~0.97	0.24	0	No
Surry RS S2-28	27 / 15	0.97~1.5	1.0	0.001	No
S2-30	27 / 15	0.97~1.5	1.3	0.10	Minor
SPS-Rig 33-C1	12/15	0.43~0.97	0.39	0	No
Millstone 2 M2-22	7 / 37.75	0.25~1.6	0.81	0.11	Minor
M2-27	7 / 37.75	0.25~1.6	0.68	0.07	Minor
Millstone 3 M3-2	8 / 30.38	0.29~1.4	5.1	0.54	**Major**
M3-16	8 / 30.38	0.29~1.4	3.6	0.54	**Major**

Response to Millstone 3, Head Loss and Vortexing, RAI 6, Issue '4b'

The above mentioned RAI 4 (NRC Request for Additional Information dated December 17, 2008) is quoted as below:

> *The explanation for higher peak head loss that occurred during large-scale strainer performance testing stated that air was released from solution when head loss across the debris bed lowered the pressure in the debris bed below the static pressure of water on top of the debris bed. This air release apparently results in higher peaks in head loss. The explanation of this phenomenon is unclear. It is also unclear as to why this phenomenon would not occur during the reduced-scale testing since the head losses and submergence were similar. Please provide additional details and evaluation of the cause of the peak head loss that occurred during this testing.*

The Millstone 3 large-scale test M3L-2 was performed in the AECL large-scale strainer testing facility—Rig 85. In that test, many air bubbles were observed coming out of the discharge header after the third fiber addition, as shown in Figure 5. The discharge header was located on the floor of the test tank.

During the test, the head loss stabilized at 2.7 psi after the second fiber addition. The third fiber addition increased the head loss to 4.1 psi. Three more fiber additions were added into the test and each addition caused a spike in head loss as shown in Figure 21. DNC's response to RAI 4, dated March 13, 2009, referred to the fourth, fifth and six fiber additions. Prior to these fiber additions, air evolution had already reached a significant level due to high debris bed head loss.

The observed head loss spike after the fourth, fifth and sixth fiber addition was due to the air bubbles trapped inside the fibrous debris. Microscopic examination of fibers prepared in a similar fashion (i.e., using a pressure washer to agitate and break up the clumps of fiber) showed that air bubbles were attached to the fibers (see Figure 22). It was the air bubbles that initiated the pressure spikes, not the fibers.

As soon as the fibers reached the debris bed, the bubbles started to migrate into the debris bed, blocking flow area and causing the head loss to increase. The increasing head loss caused the generation of more bubbles within the bed, which, in turn, caused a further increase in head loss. Once a debris addition was completed and no new bubbles were arriving at the debris bed, then the continuing migration of air bubbles through the debris bed into the fins begin to decrease, unblocking flow area and causing further head loss decreases. Eventually, the rate of air generation decreased to become equal to the rate of air migration, and the head loss stabilized at a lower value than the peak value.

Figure 21: Head Losses vs. Debris Addition in Millstone 3 Large-Scale Thin Bed Test

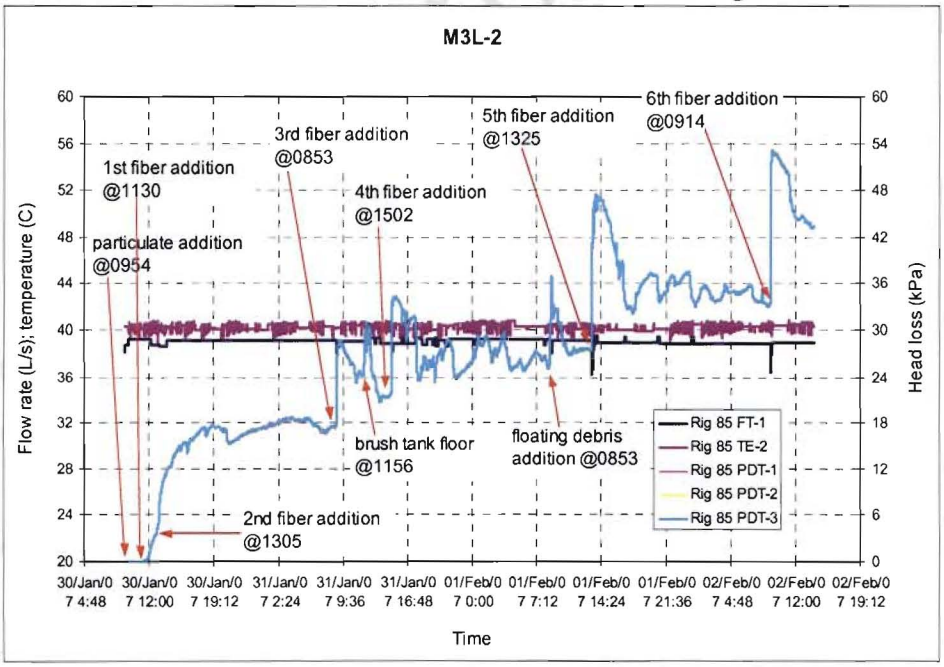

Figure 22: Air Bubbles Attached to Prepared Thermal Wrap

Fiber

Response to Millstone 3, Head Loss and Vortexing, RAI 6, Issue '4c'

As explained in response to Issue 4 b, prior to the last three fiber additions, air evolution already existed in the system due to high debris bed head loss (4.1 psi). Newly added fiber would bring entrained air bubble into the debris bed, blocking flow area and causing the head loss to increase. The increasing head loss caused the generation of more bubbles within the bed, which, in turn, caused a further increase in head loss. Once a debris addition was completed and no new bubbles were arriving at the debris bed, then the continuing migration of air bubbles through the debris bed into the fins begin to decrease, unblocking flow area and causing further head loss decreases. Eventually, the rate of air generation decreased to become equal to the rate of air migration, and the head loss stabilized at a lower value than the peak value.

Response to Millstone 3, Head Loss and Vortexing, RAI 6, Issue '5'

The head loss behavior after the chemical debris additions was explained in AECL test report MIL3-34325-TR-004 Rev 1 [22] as

> *Aluminum additions invariably resulted in head loss peaks, followed quickly by decreases in head loss. This phenomenon seems to have been the result of the addition method and may have been caused by the transiently high (and non-prototypical) concentration of dissolved aluminum. As the aluminum precipitates formed and settled, the head loss returned to lower values.*

The head loss versus time curve shown in Figure 16 demonstrated that the thin bed thickness was ¼ inch or less. As long as a thin bed was formed, further fiber addition would not increase the non-chemical debris bed head loss. Extra fiber would either loosely attach to the strainer surface forming a porous layer, or settle on the tank floor. A flow sweep at the end of the test demonstrated that the head loss responded quickly to changes in flow rate and head loss changes were found to be reversible. Post-test

examination (as shown in Figure 23) also confirmed that the debris bed was not degraded during the test and head loss was not limited by holes in, or dislocation of, portions of the debris bed.

Figure 23: A Piece of Debris Bed after the Rig-89 Testing

Response to Millstone 3, Head Loss and Vortexing, RAI 6, Issue '6'

The potential for the lower head loss in the Rig-89 testing to have been caused by agglomeration of fibrous debris was very low. Fibrous debris was sprayed as "single fine" by using a high pressure jet flow in a 200-L plastic barrel. The sprayed fiber was then added into the in-line debris addition tank. The debris addition tank was equipped with a stirrer. After a batch of fibrous debris was added into the tank, the stirrer was turned on to suspend the fiber and to avoid debris settling or agglomeration. The debris addition tank was then valved-in to let the fiber flow to the strainer box slowly by adjustment of the in-line control valves. Figure 24, Figure 25 and Figure 26 show that after the test, the debris bed was firm and uniform. No fibrous debris clumps were observed.

Figure 24: Debris Bed at the End of Millstone 3 Chemical Effects Test

Figure 25: Close-Up of a Piece of Debris Bed Removed from the Strainer Surface

Figure 26: Debris Bed Thickness after Millstone 3 Rig 89 Chemical Effects Test

Response to Millstone 3, Head Loss and Vortexing, RAI 6, Issue '7'

Assumptions:

- The RWST will be emptied within a maximum of 3 hours from the start of the accident.
- The minimum containment water level above the top of the strainer is 4.8 feet for a SBLOCA and 5.5 feet for an LBLOCA.
- The maximum temperature of the containment water is less than 185°F three hours after the accident. Water density at 185°F is 60.46 lb/ft^3.

The generation of air in the debris bed is dependent on the static head of water above the fin; if the debris bed head loss is less than the static head of water, no air evolution is expected. The submerged depth for the reduced-scale tests was set at 8 inches whereas the minimum water level in Millstone 3 containment continues to rise for 3 hours following the accident to a minimum height of 4.8 ft above the top of the strainer.

Both the maximum static head and the increase in static head with time in containment must be compared to the head loss results to determine if air could be generated in the debris bed in Millstone 3 containment.

At minimum submergence (4.8 ft), the static head at the tops of the fins in containment will be 2.0 psi with 185°F water. The maximum debris bed pressure drop was seen as 2.17 psi in Rig 89 testing. This maximum head loss value was later calculated to be 1.67 psi due to the size of the test module being 5.08 ft^2 vice the 5.74 ft^2 thought to be the surface area at the time of testing. The maximum debris bed head loss is due to addition of aluminum precipitates to the debris bed (from aluminum corrosion).

Aluminum corrosion is a long-term phenomenon which will only add particulate to the debris bed long after the water has cooled resulting in significant additional static head due to subcooling. Thus, the debris bed head loss will remain below the static head on the strainer preventing air evolution in the debris bed or strainer.

For the short-term operation, that is, within the first three hours after the accident, the static water head loss would increase to at least 2.0 psi. The sump water turnover time at the start of the RSS pump would be 57 minutes (sump water mass: 3,819,002 lb, flow rate: 8220 USGPM [23]). It only takes 3 turnovers for the static water head to reach at least 2.0 psi. The Rig 89 test turnover time was 5 minutes. As can be seen from Figure 1, 3 turnovers (15 minutes) after the first fiber addition, the debris bed head loss could barely reach 0.1 psi. As observed in the strainer testing, it usually took days to build a thin bed. Thus, for the short-term operation, air evolution could not occur in the plant strainers.

Due to non-prototypical test conditions, such as biological growth, river water particles and air evolution, the non-chemical head loss determined in the Rig 33 test was not representative and thus should not be used for air evolution evaluation for the plant strainers.

Millstone 3, Net Positive Suction Head, RAI 9

It is not clear how water drains from the refueling cavity into the reactor cavity, and whether this drainage path is large enough to ensure that debris blockage would not occur. While the plant Final Safety Analysis Report (FSAR) documents that a significant amount of venting surface is available, there is also a significant quantity of debris available. The potential for blockage of the vent covers is also considered in the FSAR.

The RAI intended to ask about the entire refueling cavity: did your response account for the entire refueling cavity or only the cavity saddle? If your RAI response did not account for the entire refueling cavity, please update your response.

To ensure that the evaluation has accounted for the worst-case minimum containment water level, please clarify the drainage path from the refueling cavity to the reactor cavity, the minimum flow restrictions, and provide a basis for why blockage would not occur there.

Response to Millstone 3, Net Positive Suction Head, RAI 9

The previous RAI response (see Attachment 2 to DNC Letter Serial 09-175 dated March 13, 2009) considered the maximum potential holdup volume of the refueling cavity. The minimum water level calculation conservatively determines the minimum containment water level which exists at the earliest RSS pump start time. The total possible holdup in the refueling cavity is limited to 49,202 gallons since any water beyond this volume spills into the reactor cavity and instrumentation tunnel which in turn spills over to the containment floor. The instrumentation tunnel is assumed to be full and the refueling cavity is considered to be 99% full (48,823 gallons) in determining the minimum sump water level.

Water spills from the refueling cavity into the reactor cavity through open Seal Ring Hatches. Spillover through the eight (8) Seal Ring Hatches (each about 24-inch diameter) directly enters the reactor cavity and spills into the instrument tunnel prior to reaching the containment floor. Seal Ring Hatch Protective Covers are installed over the open Seal Ring Hatches (raised 8.5-inch above the opening). These covers allow unimpeded air and water flow during plant operation. The open Seal Ring Hatches with protective covers installed do not present credible locations for debris blockage due to the large size of the openings. No other minimum flow restrictions between the refueling and reactor cavities exist.

Millstone 3, Chemical Effects Questions

AECL performed dissolution tests both with and without tri-sodium phosphate (TSP) in the beakers. The testing showed that the tests that included TSP showed an inhibition of the calcium dissolution. However, for the head loss testing the licensee stated that they applied the calcium quantity determined by the uninhibited (non-TSP) bench testing. Data from the lowest allowable pH (7.0) was used when determining the amount of calcium to be added to the head loss test. The calcium concentration used for head loss testing was 14.7 mg/L. This value is significantly lower than the measured value for the 30-day bench scale dissolution testing, which used scaled amounts of concrete to represent the MPS3 condition. Please provide the following additional information in order to determine that the testing was performed in an acceptable manner:

14. *The solubility data for calcium shows increased dissolution at lower pH ranges. In table 0-2, Attachment 2, to the December 18, 2008 letter, the calcium concentrations for pH 5.0 and 6.0 are lower than the concentration for pH 7.0. In addition, page 11 of 30 states that the concrete samples in the beaker tests fully dissolved in the pH 5.0 and 6.0 tests but were not fully dissolved in the pH 7.0 and 8.0 tests. Please explain why the bench tests at lower pH ranges, in which the concrete fully dissolved, resulted in lower concentrations of dissolved calcium than the bench tests at higher pH ranges, in which the concrete did not fully dissolve.*
15. *For MPS3, the calcium dissolution test at pH of 7.0 resulted in a 30-day calcium concentration of 78 mg/L. The December 18, 2008, letter states that the pH 7.0 case (without TSP present) was used to determine the concentration of calcium in the Rig-B9 test. However, the calcium concentration used for Rig-89 testing was 14.7 mg/L. Please justify why 14.7 mg/L is a representative value in the Rig-89 testing when the dissolution testing conducted with scaled quantities of concrete resulted in a calcium concentration of 78 mg/L.*
16. *DNC's testing was performed at 104^{0}F, which is well below early post-loss-of-coolant accident pool temperatures. The solubility of calcium phosphate (hydroxyapatite) decreases as the temperature increases. Please discuss whether more calcium phosphate precipitate would have formed in the Rig-89 tests if this test would have been performed at higher temperature. If more calcium phosphate precipitate would be expected at a higher temperature, when the short-term NPSH margin is applicable, please justify why the overall Rig-89 test results provide for an adequate evaluation of chemical effects.*

17. *Please compare the total amount of aluminum that is predicted to be released by the AECL model with that predicted by the WCAP-16530 base model (i.e., no refinements for silicate or phosphate inhibition). Discuss any significant differences between the plant-specific predictions for the two methods, including the acceptability of these differences.*

Response to Millstone 3, Chemical Effects Question 14

The coupons used in these tests were small and subject to variability of rock and mortar content; thus, it must be argued that the coupons used in the pH 5 and 6 tests contained less mortar (the primary source of calcium) than those used in the pH 7 and 8 tests. The slightly lower concentrations attained in the pH 5 and 6 tests represented the limit of the calcium source (mortar) while slightly higher concentrations were attained in the pH 7 and 8 tests, despite the coupons remaining structurally intact. A more detailed explanation of the apparent conflict between the results of these tests and calcium solubility data is included below.

Concrete is inherently basic, and experts and literature agree that concrete dissolution rates increase as the exposed medium becomes more acidic. In the AECL Test Report [24] of bench-top tests conducted for Dominion, the results of dissolution tests simulating the Millstone 3 concrete surface area-to-volume ratio[5] do show higher dissolution rates at lower pH ranges, but the ultimate concentrations reached were lower in the tests at pH 5 and 6 than in those at pH 7 and 8 (Figure 27). This apparent contradiction can be explained by the small size of the coupons used: each coupon measured approximately 0.4×1.2×0.5 cm, and were small in comparison to similar tests performed for Millstone 2. As a result of their limited size, two of the coupons completely dissolved in the pH 5 and 6 tests. As well, their small size made them more prone to containing non-uniform proportions of rock and mortar. Consequently, the calcium concentrations measured toward the end of the pH 5 and 6 tests represent the natural limit when all of the concrete had dissolved. The data from all of the tests were fit to Equation 6. The early plateau seen in Figure 27 for the pH 5 and 6 tests biased their extrapolated concentrations at t=∞ shown in Table 7 (Table O-2 of the above-mentioned letter).

$$Ca\ Release\ (t) = C_{\infty}(1 - \exp(-kt))$$

Equation 6

Table 7: Calcium Concentration Fitting Parameters of Equation 6 from Millstone 3 Dissolution Tests

Parameter	pH 5	pH 6	pH 7	pH 8
C∞ [mg/L]	82	77	103	68
k [h^{-1}]	0.017	0.0049	0.0029	0.0034

[5] As estimated at the time; the ratio has since changed.

Figure 27: Calcium Release Data from Millstone 3 Dissolution Tests without TSP at 90°C

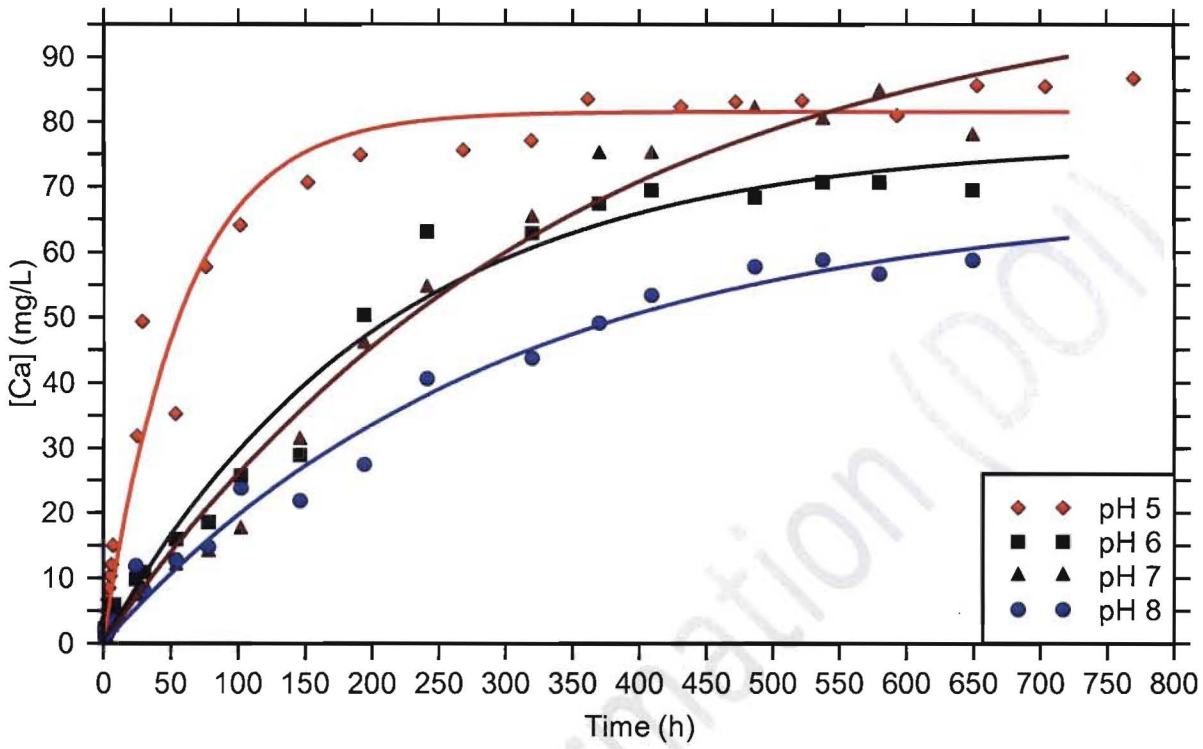

Note the lines are fits of the data sets to a first-order release equation.

The recovery of coupons from the pH 7 and 8 tests, and the lack of any obvious plateau in Figure 27, strongly implies that the results of these more important tests were not biased by a limited calcium source. The results of the pH 7 test, in particular, were used in the design of reduced-scale test, as pH 7 is the minimum allowed sump water pH. However, it should be noted that this remains a conservative estimate of calcium release since the Millstone Unit 3 sump is likely to remain mainly above pH 8.

Response to Millstone 3, Chemical Effects Question 15

The value of 14.7 mg/L used in the Rig 89 testing was calculated by appropriately scaling the results of the dissolution tests to match updated estimates of the Millstone 3 concrete surface area. This response will show:

1. The concrete surface area-to-volume ratio used in the bench-top dissolution tests was based on estimates of the concrete surface area that were later updated;
2. The results of the dissolution tests may be normalized to units of calcium release per unit area, which may then be used to calculate the expected calcium release and calcium concentration in Millstone 3 based on the updated concrete surface area;
3. It is appropriate to use the fit to the entire data set to determine the scaled calcium concentration rather than to scale the analysis result obtained on day 30 (78 mg/L), which is more subject to sampling and statistical errors.

The concrete surface area-to-volume (SA/V) ratio used in the bench-top dissolution tests was roughly 6 times greater than the current calculated SA/V ratio using data from ERC 25212-ER-06-0013 Rev. 2 [23] and leads to the apparent discrepancy. The dissolution tests conducted from February to March, 2008, used coupons sized to meet the SA/V ratio calculated from Rev. 1 of that document [25] and included scaled quantities of fibrous debris. Table 8 compares the SA/V ratio used in the dissolution tests to those calculated from the source references. It is important to note that, by design, there is no uncoated concrete within the Millstone 3 containment and that all values quoted are conservative estimates of bare areas exposed either by chipping and wear or by impact of the break jet [23].

Table 8: Comparison of Dissolution Test Concrete SA/V Ratio to Millstone 3 Values

Source	ERC 25212-ER-06-0013 Rev. 1	Dissolution Test	ERC 25212-ER-06-0013 Rev. 2
Date	2007/09	2008/02 – 2008/03	2008/04
Submerged Concrete	1000 ft^2 (9.29×10^5 cm^2)	0.4×1.2×0.5 cm coupons (2.56 cm^2)	100 ft^2 (9.29×10^4 cm^2)
Exposed Concrete	1932 ft^2 (1.795×10^6 cm^2)	-	408 ft^2 (3.79×10^5 cm^2)
Volume	3,819,002 lb_m @61.55 lb_m/ft^3 (1.757×10^6 L)	4 L	160,000 ft^3 (4.53×10^6 L)
SA/V Ratio (Submerged)	0.529 cm^2/L	0.64 cm^2/L	0.0205 cm^2/L
SA/V Ratio (Total)	1.55 cm^2/L	-	0.104 cm^2/L

Because the concrete SA/V ratio for containment differs from that tested, the results obtained are non-representative but may be appropriately scaled. Normalization of the dissolution test data may be performed by dividing the results (in mg/L) by the SA/V ratio (0.64 cm2/L), as indicated by the right-hand vertical axis in Figure 28. Similarly, the fit to the calcium concentration data, described below, may also be normalized to produce a calcium release equation. Thus, the 30-day calcium release per unit area of concrete can be read from the figure or calculated from the fit and used to calculate the calcium release from a known surface area of concrete.

Figure 28 also shows the curve fits to the data represented by Equations 7 and 8. These were determined using robust fitting procedures within TableCurve 2D[†] that reduce the fitting errors caused

[†] TableCurve 2D is produced and distributed by Systat Software Inc.

by data outliers. The constants found within Equation 7 were reported in Table 2-5 of the bench-top Test Report [24] and Table O-2 of DNC's December 18, 2008 letter. Equation 8 may be calculated from Equation 7 by dividing the initial constant[6] by the tested surface area-to-volume ratio, 0.64 cm^2/L.

$$Ca\left[\frac{mg}{l}\right] = 103\left[\frac{mg}{L}\right](1 - exp(-0.0029h^{-1}t)) \quad \text{Equation 7}$$

$$Ca\ Release\left[\frac{mg}{cm^2}\right] = 160\left[\frac{mg}{cm^2}\right](1 - exp(-0.0029h^{-1}t))$$

Equation 8

Figure 28: Calcium Release Data @ Millstone 3 pH 7, pH 8 Dissolution Tests w/o TSP @ 90°C

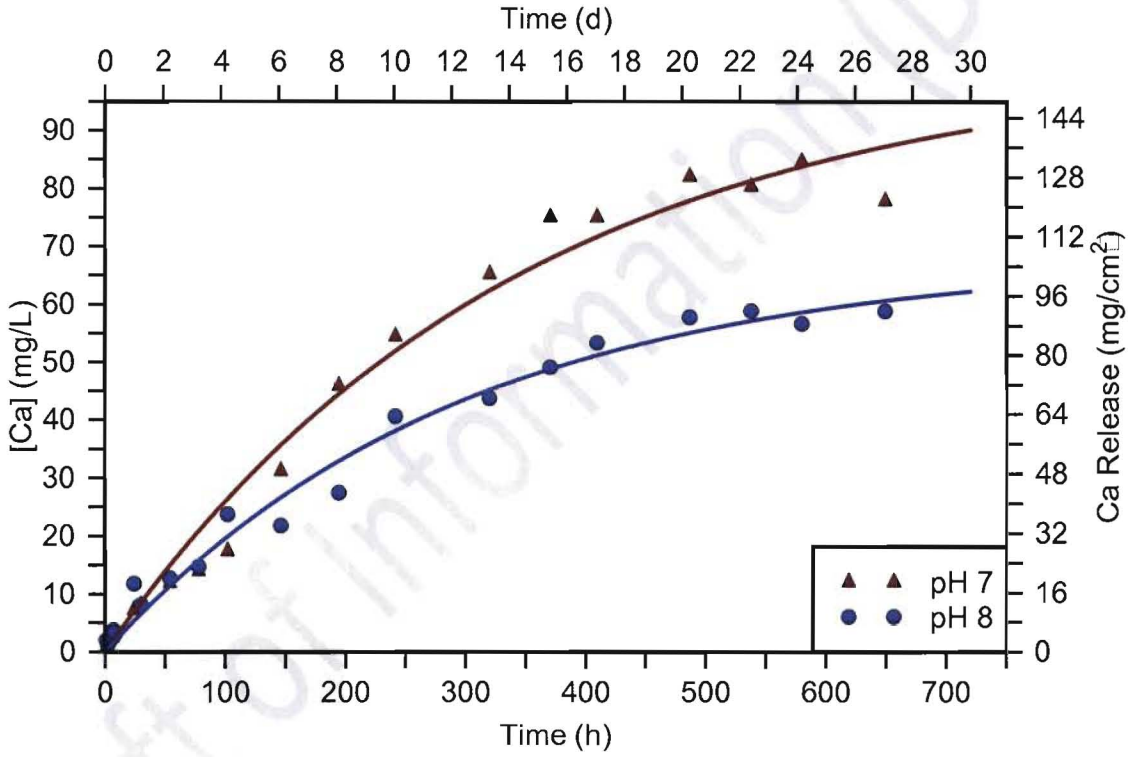

Note the lines are fits of the data sets to a first-order release equation.

It is appropriate to use the fit rather than the raw data to determine the 30-day calcium concentration, as drifts in pH, sampling errors, and statistical error associated with the analysis technique, ICP-OES (Inductively Coupled Plasma Optical Emission Spectroscopy), may alter the measured concentration.

After 30 days, the expected calcium release at pH 7 and 90°C:

---

[6] The initial constant, C_∞, was determined to be 102.5 mg/L, where the tenths decimal place should not be considered significant.

$$Ca\ Release\ \left[\frac{mg}{cm^2}\right] = 160\left[\frac{mg}{cm^2}\right](1 - \exp(-0.0029h^{-1} \cdot 720h)) = 140\left[\frac{mg}{cm^2}\right]$$

Using the SA/V ratio from the 4th column of Table 8, 0.104 cm^2/L, the expected calcium concentration is:

$$Ca\ Expected\ \left[\frac{mg}{L}\right] = 140\ \left[\frac{mg}{cm^2}\right] \cdot 0.104\left[\frac{cm^2}{L}\right] = 14.6\left[\frac{mg}{L}\right]$$

For comparison, the expected calcium concentration at pH 8 is 10.1 mg/L by similar analysis.

This result may be compared to the WCAP method of calculating calcium release, as described by Lane et al [8]. In utilizing this method, the calculated pH has been used; in order to maximize the release rate, the maximum pH was used to calculate the release from Transco Thermal Wrap (around pH 8.1) and the minimum pH was used to calculate the release from concrete (around pH 8.0). By this method, the calculated calcium release from concrete is miniscule[7]; most of the calcium released comes from fibrous debris. The calcium concentration is predicted to plateau at 10.6 mg/L (Figure 29), the "saturation limit" of calcium released from Transco Thermal Wrap at pH 8.1 and 165.34°F (74.08°C). Therefore, the calcium concentration obtained by scaling the AECL pH 7 dissolution test results is conservative with respect to the WCAP result.

Figure 29: Calcium Release from Millstone 3 Fibrous Debris/Concrete IAW WCAP Method

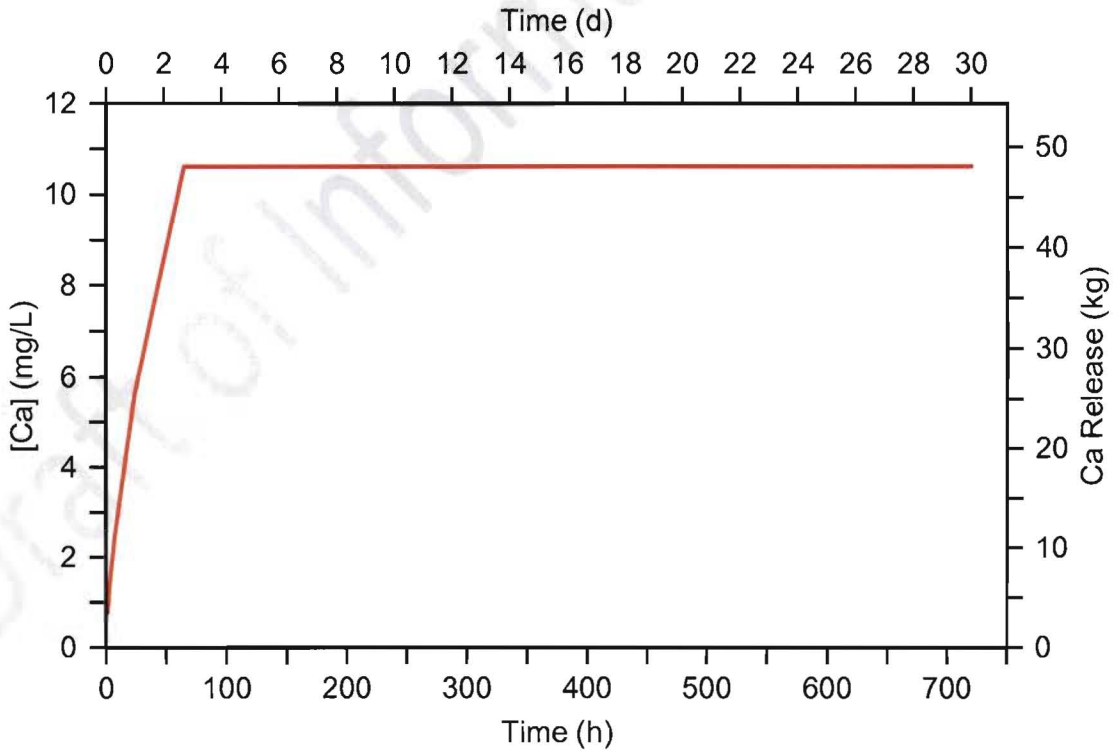

[7] When the Transco Thermal Wrap contribution to calcium release is neglected, the calculated calcium release from concrete using the WCAP method is less than 5 g. By contrast, when the Transco Thermal Wrap contribution is included, the calculated calcium release is nearly 50 kg.

Response to Millstone 3, Chemical Effects Question 16

This response will show that:

1. Literature data suggest the solubility of calcium phosphate increases above some minimum temperature around 60°C
2. A large degree of supersaturation was observed during the tests, suggesting that kinetic factors play a large role in the quantity of precipitate

With these points in mind, it is argued that the Rig 89 test results provide an adequate evaluation of chemical effects.

Calcium Phosphate Solubility

Calcium and phosphate ions can form a variety of low solubility salts in aqueous solution depending on the temperature, ions present (and therefore ionic strength), pH and the Ca/P ratio in the solution. The typical sparingly soluble calcium phosphates, which are relatively stable in aqueous systems, are hydroxyapatite, $Ca_5(PO_4)_3OH$, whitlockite, β-$Ca_3(PO_4)_2$, octacalcium phosphate, $Ca_8H_2(PO_4)_6{\cdot}5H_2O$, monetite, $CaHPO_4$, and brushite, $CaHPO_4{\cdot}2H_2O$. The solubility of these phases has been typically measured around ambient temperature; the reported results, including the solubility product constants, can differ significantly from group to group.

Of the possible calcium phosphate phases, hydroxyapatite has been found to be the least soluble in water above pH 4 and the thermodynamically most stable phase of calcium phosphate. When the solubility of calcium phosphate is the factor that limits the concentration of calcium or phosphate ions in solution, it is usually expected that hydroxyapatite is the first phase to precipitate from a solution saturated with respect to its solubility. However, experience shows that $CaHPO_4{\cdot}2H_2O$ and $Ca_8H_2(PO_4)_6{\cdot}5H_2O$ can also precipitate, particularly at ambient temperatures, and the degree of supersaturation with respect to hydroxyapatite is sufficiently high that their solubilities are also exceeded. These precipitated salts tend to transform to more stable phases such as hydroxyapatite but the process may be slow, illustrating the important role played by kinetic factors.

Sparingly soluble calcium phosphates appear to show different dissolution behavior at low and high temperatures. Below 50°C, calcium phosphate solubilities decrease with increasing temperatures. At higher temperatures, above 150°C, the limited experimental data from conductivity measurements and solubility experiments show that dissolved calcium and phosphate concentrations increase with increasing temperatures. Solubility data for calcium phosphates between 40 and 100°C, which are particularly relevant to understanding the potential for precipitation in post-LOCA sump water, are not available. However, the data indicate that there is a solubility minimum between 50 and 150°C, probably around 60°C based on the extrapolation of experimental data shown in Figure 30.

Figure 30: Dissolved Calcium Concentration in Equilibrium with Hydroxyapatite at pH 7

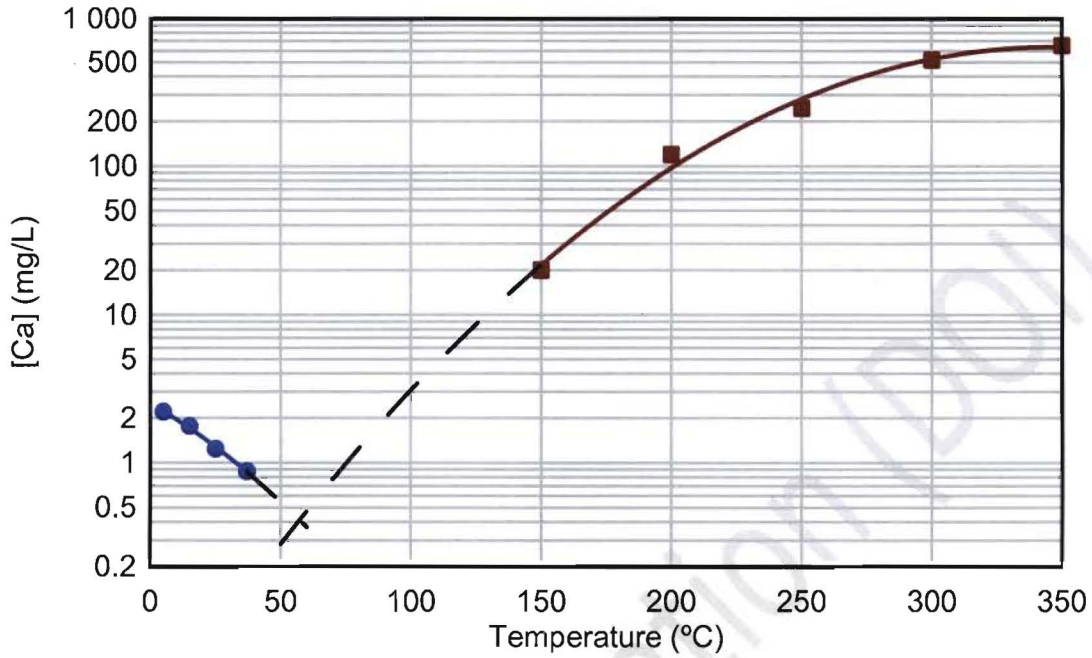

Note the data above 150°C were reproduced from Zhang et al [9]. The data below 50°C were calculated by extrapolation of the data of McDowell et al [10]. Solid lines represent experimental data; the dashed line is extrapolated.

For the first two hours following a LOCA, when temperatures could approach 212°F (100°C) and calcium release from the various sources should not exceed 1 mg/L[8], the solubility from Figure 30 is predicted to be about 3.5 mg/L and therefore calcium phosphate is not expected to precipitate.

Kinetic Factors Observed to Affect Precipitation

The reduced-scale tests performed in Rig 89 were conducted at 40°C (104°F), pH 7 and 6600 mg/L TSP, and though the highest concentration observed was 15.1 mg/L Ca, there were no indications of a solubility limit being reached: each addition resulted in a corresponding increase in calcium concentration. Note that this concentration is about 19 times greater than the hydroxyapatite equilibrium concentration (Figure 30) and above the concentration calculated for Millstone 3 by the WCAP method, 10.6 mg/L. Figure 31 shows the measured calcium concentration, which was observed to increase directly with the amount of calcium before aluminum additions began.

[8] Based on the WCAP method of calculating calcium release. By Equation 6, the release is calculated to be 0.93 mg/cm^2 or 0.10 mg/L.

Figure 31: Calcium Concentration in Rig 89 Reduced-Scale Tests vs. Calcium Added

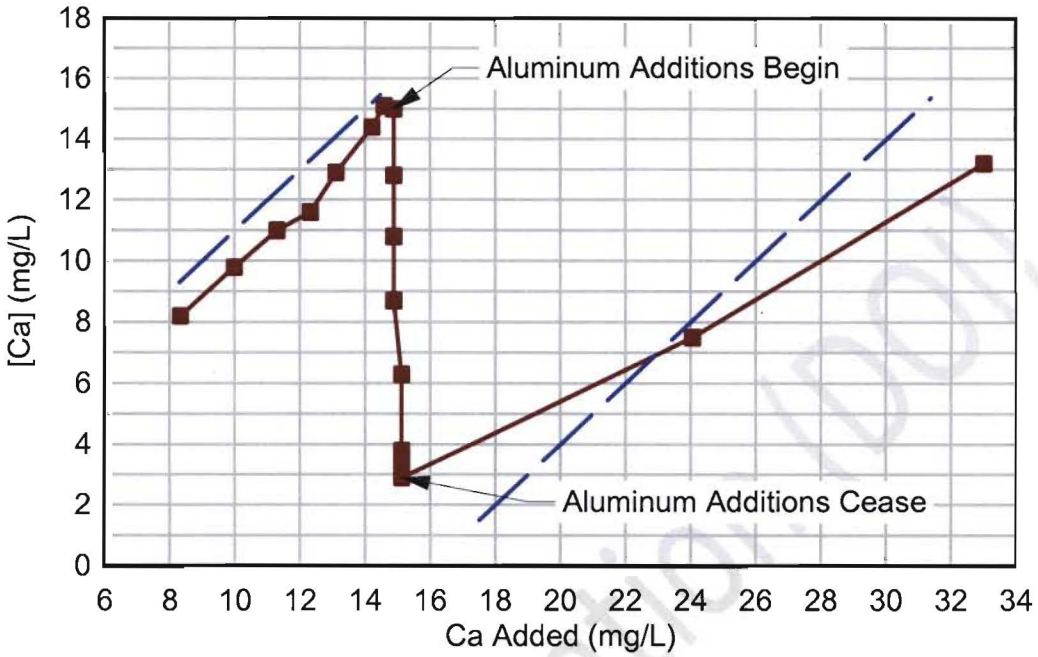

Note a maximum concentration of 15.1 mg/L Ca was observed. By comparison to the dashed lines that indicate a slope = 1, it can be seen that calcium additions resulted in a direct increase in calcium concentration before aluminum additions began. Aluminum additions were observed to reduce calcium concentration, suggesting co-precipitation.

Summary

If Rig 89 tests were performed at higher temperature, e.g., at an early post-LOCA temperature such as 100°C or a longer-term temperature such as 75°C, the available data (Figure 30) suggest that the solubility should be greater and there should be less precipitation. Furthermore, the results of the test show that the solution is stable with respect to precipitation at concentrations greatly exceeding the calculated solubility, likely as a result of kinetic factors. Thus, the Rig 89 tests provide an adequate evaluation of chemical effects and therefore show that worst-case head loss remains within available NPSH margin.

Response to Millstone 3, Chemical Effects Question 17

The WCAP-16530 base model is an empirical model of the aluminum release rate (RR) based on the data set described by Lane et al [8], which included data from ICET 1, CR-6873, WCAP-7153A and WCAP-16530. The WCAP model is described by the Equation 9 and the results are shown in Figure 32.

$$RR\left[\frac{mg}{m^2 \cdot min}\right] = 10^{14.69039 - 4.64537\left(\frac{1000}{T(K)}\right) + 0.044554(pH_a)^2 - \frac{1.20131 pH_a T}{1000}}$$

Equation 9

Figure 32: 3D Illustration of the WCAP Aluminum Release Model

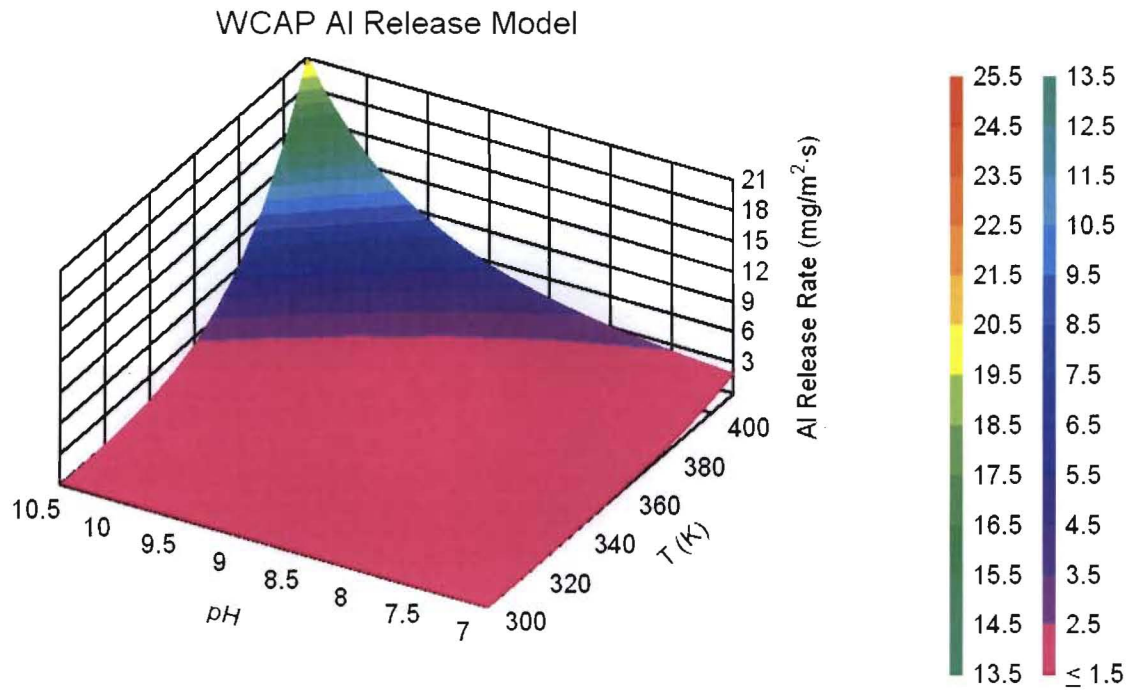

The AECL model is a semi-empirical model of the aluminum release rate, in that the equation form was developed from first principles but the parameters were fit to literature data. The release equation takes an Arrhenius form with temperature and, since the corrosion reaction involves hydroxide, the release rate is likewise related to the exponential of the pH. The data set used to fit the model was described by Guzonas and Qiu [26] and was very similar to that used for the WCAP-16530 model. The AECL model is described by Equation 10 and the results are shown in Figure 33.

$$RR\left[\frac{mg}{m^2 \cdot s}\right] = 55.2\exp\left(1.3947pH - \frac{6301.1}{T(K)}\right)$$

Equation 10

Figure 33: 3D Illustration of the AECL Aluminum Release Model

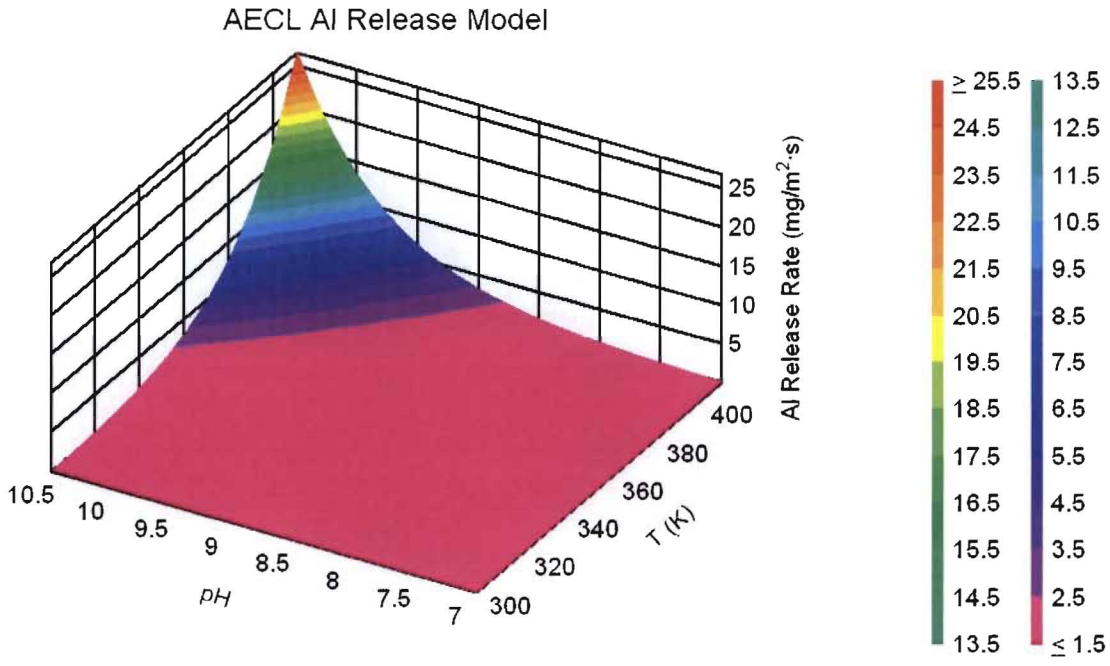

Both models ignore any time dependence of the Al release rate. As one might expect, the two models give similar predictions. Mathematical comparison of the two models shows that they differ mainly at temperatures above the normal boiling point of water. The WCAP model predicts higher release at moderate pH values (between pH 7-9.5) and lower release at high pH values, as shown in Figure 33. At more moderate temperatures, the two models predict very similar release rates. For example, ICET Test 5 [11] was conducted at 60°C at pH 8.0-8.5, and both models are observed to conservatively predict the long-term aluminum release, especially when release from sprayed aluminum with high-pH spray is included (Figure 34).

Figure 34: 3D Differential of WCAP and AECL Aluminum Release Models

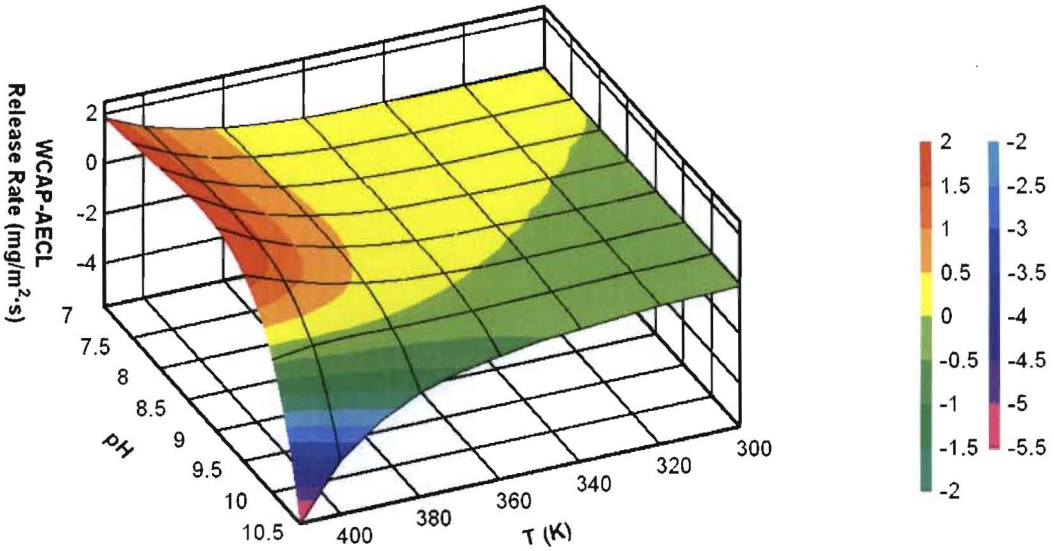

Figure 35: WCAP/AECL Aluminum Release Model of ICET Test 5 Aluminum Concentration

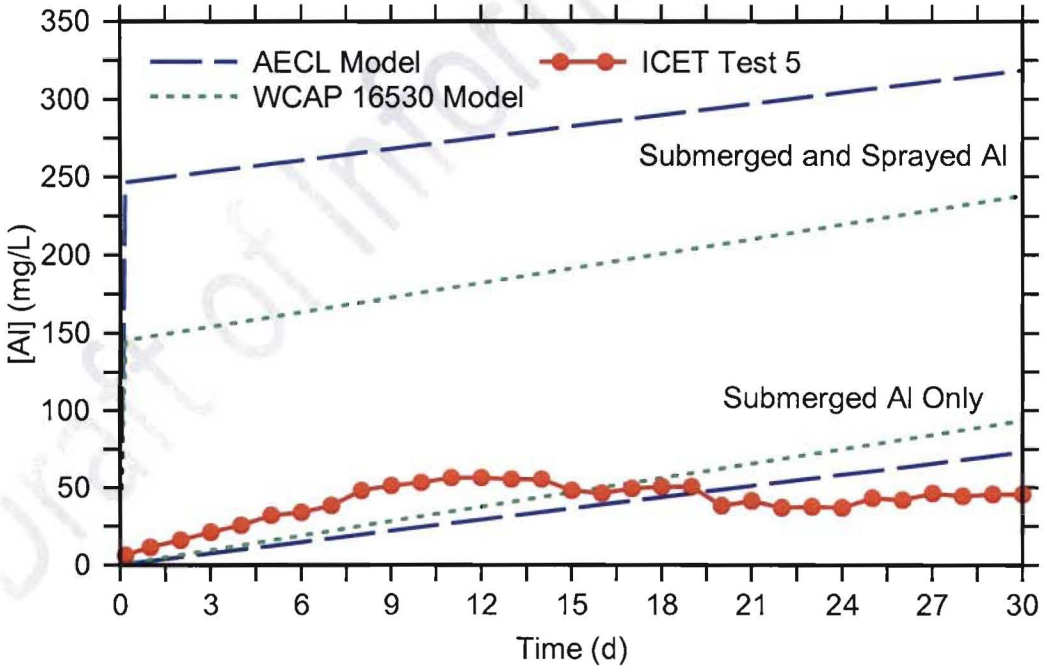

Note ICET Test 5 concentration data adapted from [11]. Spray pH, reported as < 12, was taken to be 11 for calculations.

The Millstone 3 post-LOCA sump and spray operates mainly in the range of pH 8.0-8.5, where the WCAP model predicts a greater aluminum release rate at high temperatures than the AECL model (Figure 36). For the 1080 ft^2 of sprayed and 120 ft^2 of submerged aluminum reported to be present at Millstone Unit 3 [23], the WCAP model predicts 14.6 kg Al whereas the AECL model predicts 8.15 kg Al (Figure 36). Note that the scaled equivalent of 7.6 kg Al was added during the Rig 89 test[9] and that the last 2 aluminum additions (i.e., additions 11 and 12, Figure 37), representing over 30% of the aluminum added, did not produce increases in head loss, suggesting a head loss plateau. Although slightly more aluminum was needed to meet the predicted aluminum release, the observed head loss plateau allows confident prediction of the head loss for the predicted aluminum release.

Figure 36: Comparison of AECL/WCAP Aluminum Release Model of the Submerged, Sprayed and Total (Combined) Aluminum Release for Millstone 3 Post-LOCA

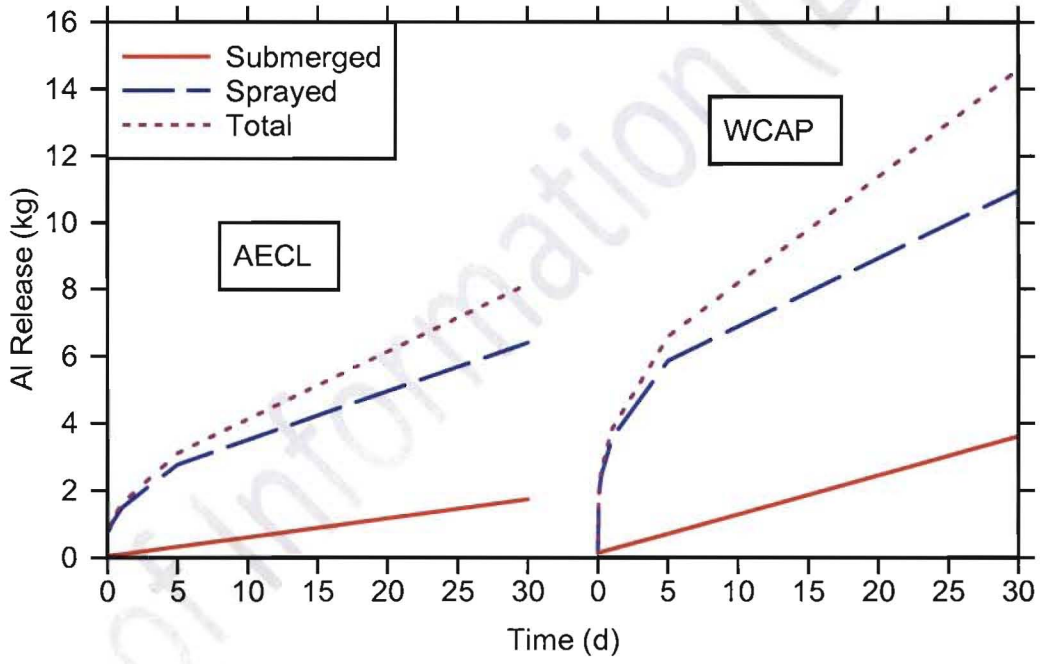

Containment

[9] Although the scaled equivalent of 7.6 kg of Al was added during the test, only 7.45 kg can be said to have precipitated with certainty due to the error uncertainty resulting from the method detection limit for ICP-OES for aluminum (0.4 mg/L)

Draft of Information (DOI) – This DOI is entirely preliminary and used solely to support teleconferencing to affirm a common understanding of the scope and intent of several NRC questions. This DOI provides draft responses to the requests for additional information and, accordingly, the information provided should not be used as part of any NRC final decision making regarding this topic.

Figure 37: Rig-89 Head Loss Trace Corrected to Match Approach Velocity of Millstone Unit 3

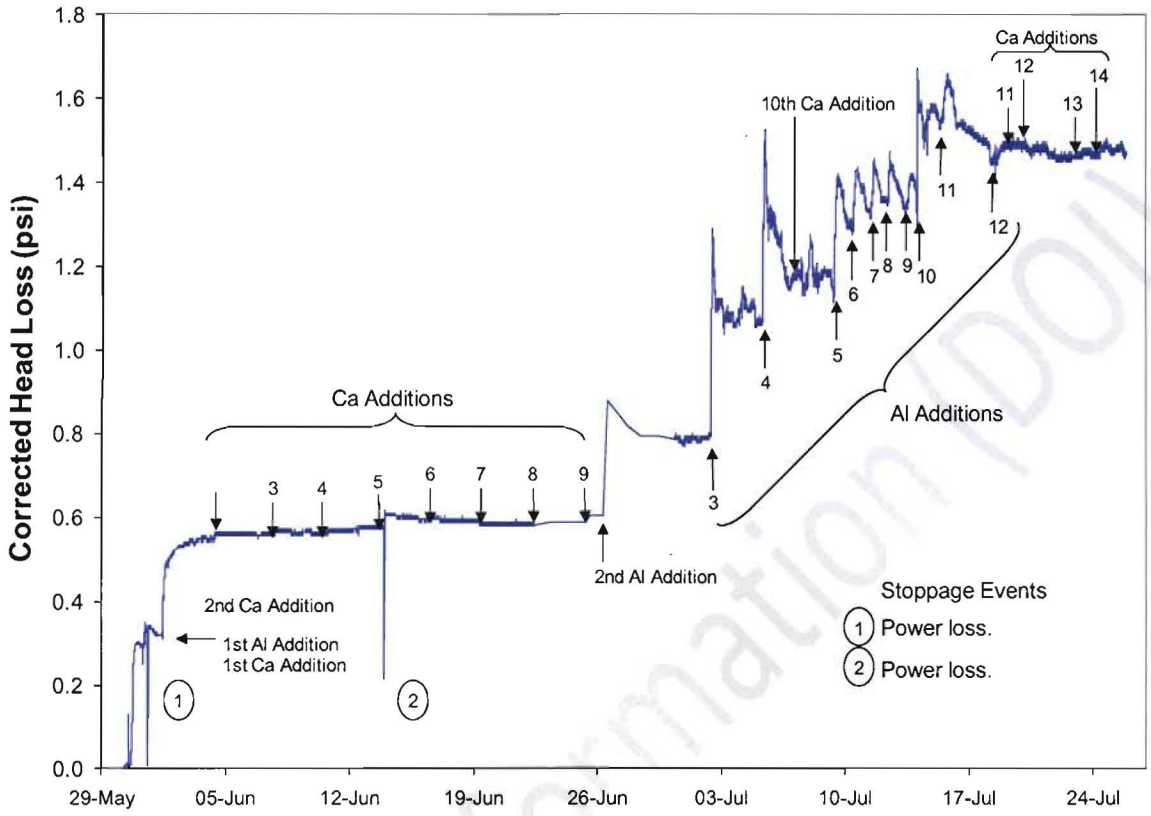

Without 30-day aluminum corrosion tests where temperatures (and pressures) of the Millstone 3 sump are simulated, it is difficult to speculate on the significance of the difference between predictions of the WCAP and AECL models. The only available data for aluminum release at pH 8 for temperatures exceeding the normal boiling point of water was reported for a 90-minute test at 265°F (129°C) by Lane et al [8]; the reported release rate of 6.6 mg/(m^2·s) was many times greater than that predicted by either model (the WCAP model predicts 2.7 mg/(m^2·s), and the AECL model predicts 1.0 mg/(m^2·s)). While this comparison may seem to highlight apparent deficiencies in both models, the deficiencies of the data set are more apparent, as it cannot be said with any certainty that the value of 6.6 mg/(m^2·s) is either accurate or repeatable. There are many variables to control in corrosion tests, and it is difficult to get consistent results; hence, Lane et al [8] could measure a release rate of 0.75 mg/(m^2·s) at pH 8 and 190°F (88°C) while others could measure lower rates at more severe conditions: Reid et al [12] measured 0.13 mg/(m^2·s) at pH 8 and 200°F (93°C), Bell et al [13] measured 0.20 mg/(m^2·s) at pH 8 and 210°F (99°C), and Jain et al [14] measured 0.53 mg/(m^2·s) at pH 10 and 194°F (90°C). These values are compared to WCAP and AECL model predictions at pH 8 in Figure 38. It is clear there is a large scatter in the test data, with two data points clustered closely together and one very much higher. This may reflect differences in test methodology or conditions; AECL has found experimental uncertainties of about 30% in nominally identical tests. Both models predict release rates within the scatter of the plotted data; the AECL model better fits most of the data, but the WCAP model more closely models the

average value and is the more conservative. However, the limited experimental data available do not provide a basis for selecting one model over the other, and no significance can be ascribed to the differences in the predicted aluminum release.

Figure 38: Comparison of AECL and WCAP Aluminum Release Model Predictions and Measured Values at

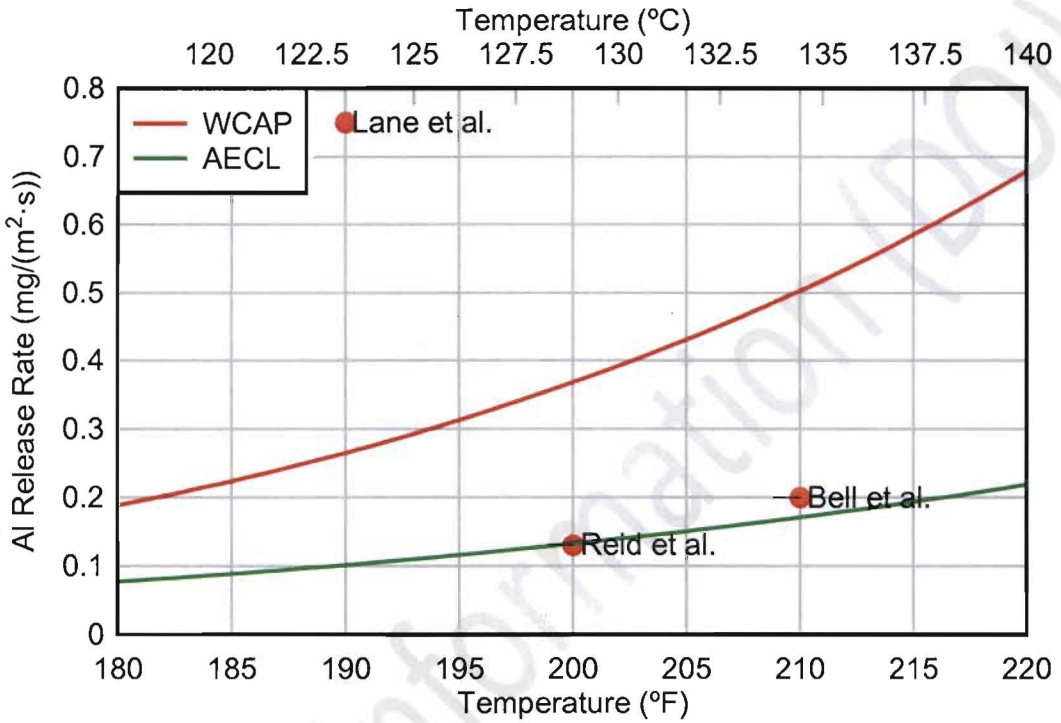

pH 8

It should also be noted that neither model was developed to predict short-term release rates. Although short-term release rates may be higher than predicted by the models, long-term release rates are likely to be lower than predicted, as indicated by the results of ICET Test 5 (Figure 35) and other tests showing a plateau in release rates, including the classic aluminum corrosion tests described by Troutner [15, 16].

References

[1] Fisher NJ, Bartlett MM, Cheng Q. Reduced-scale testing for Millstone 2 replacement containment sump strainers. AECL Test Report MIL2-34325-TR-001, Rev. 0; 2006 September.

[2] Fisher NJ, Bartlett MM, Cheng Q. Large-scale testing for Millstone 2 replacement containment sump strainers. AECL Test Report MIL2-34325-TR-002, Rev. 0; 2006 October.

[3] Legg M. Millstone Unit 2 inputs for GSI-191 strainer head loss testing. Dominion ERC No.: 25203-ER-07-0029, Rev. 0; 2007 December 20.

[4] Guzonas D, Edwards MK, Cheng Q, Haque Z, Deadman J. Final report on strainer debris bed head loss arising from prototypical chemical addition: Dominion: Millstone 2. AECL Report No.: MIL2-34325-TR-004 Rev. 1; 2009 October.

[5] Legg M. Millstone Unit 2 inputs for GSI-191 chemical effects testing. Dominion ERC No.: 25203-ER-06-0007, Rev. 3; 2008 Apr 15.

[6] Legg M. Millstone Unit 2 inputs for GSI-191 chemical effects testing. Dominion ERC No.: 25203-ER-06-0007, Rev. 1; 2007 Aug 21.
[7] Guzonas D, Qiu L, Edwards M. Results of bench-top chemical effects tests: Dominion – Surry 1 and 2, North Anna 1 and 2, Millstone 2 and 3. AECL Report No.: DOM 34325-TR-001 Rev. 0; 2008 July.
[8] Lane AE, Byers WA, Jacko RJ, Lahoda EJ, Reid RD. Evaluation of post-accident chemical effects in containment sump fluids to support GSI-191. Westinghouse Report No.: WCAP-16530-NP-A; 2008 March.
[9] Zhang H, Li S, Yan Y. Dissolution behaviour of hydroxyapatite powder in hydrothermal solution. Ceramic International. 2001;27:451.
[10] McDowell H, Gregory TM, Brown WE. Solubility of $Ca_5(PO_4)_3$ in the system $Ca(OH)_2$-H_3PO_4-H_2O at 5, 15, 25, and 37°C. Journal of Research of the National Bureau of Standards-A, Physical and Chemistry. 1977;81A:273.
[11] Dallman J, Letellier B, Garcia J, Madrid J, Roesch W, Chen D, Howe K, Archuleta L, Sciacca F, Jain BP. Integrated chemical effects test project: Consolidated data report. NUREG/CR-6914; 2006 August.
[12] Reid RD, Crytzer KR, Lane AE. Evaluation of additional inputs to the WCAP-16530-NP chemical model. Westinghouse Report No.: WCAP-16785-NP; 2007 May.
[13] Bell MJ, Bulkowski JE, Picone LF. Investigation of chemical additives for reactor containment sprays. Westinghouse Report No.: WCAP-7153A; 1975 April.
[14] Jain V, He X, Pan YM. Corrosion rate measurements and chemical speciation of corrosion products using thermodynamic modeling of debris components to support GSI-191. U.S. NRC Report NUREG/CR-6873; 2005 April.
[15] Troutner VH. Observations on the mechanisms and kinetics of aqueous aluminum corrosion: Part 1—role of the corrosion product film in the uniform aqueous corrosion of aluminum. Corrosion. 1959; 15(1):9t-15t.
[16] Troutner VH. Uniform aqueous corrosion of aluminum—effects of various ions. Hanford Atomic Products Operation Report No.: HW-50133; 1957 June 10.
[17] Fisher, N.J., Cheng, Q. and Haque, Z., "Reduced-Scale Testing for Surry 1 and 2 Replacement Containment Sump Strainers", AECL Test Report SUR2-34325-TR-001, Rev. 0, 2007 November.
[18] Fisher, N.J., Bartlett, M.M. and Cheng, Q., "Reduced-Scale Testing for Millstone 3 Replacement Containment Sump Strainers", AECL Test Report MIL3-34325-TR-001, Rev. 0, 2007 March.
[19] Manson, R.E., Ophel, I.L., "Experience with Slime Forming Organisms in Chalk River Reactor Systems", AECL Report 1124, 1960 September.
[20] Fisher, N.J., Cheng, Q. and Haque, Z., "Reduced-Scale Testing for North Anna 1 and 2 Replacement Containment Sump Strainers", AECL Test Report NAN2-34325-TR-001, Rev. 1, 2008 February.
[21] Cheng, Q., Fisher, N.J., Bartlett, M.M., Haque, Z., "Large-Scale Testing for Millstone 3 Replacement Containment Sump Strainers", AECL Test Report MIL3-34325-TR-002, Rev. 0, 2007 April.
[22] Edwards MK, Cheng Q, Guzonas D, Haque Z, Final report on strainer debris bed head loss arising from prototypical chemical addition: Dominion: Millstone 3. AECL Report No.: MIL3-34325-TR-004 Rev. 1; 2009 October.
[23] Legg M. Millstone Unit 3 inputs for GSI-191 chemical effects testing. Dominion ERC No.: 25212-ER-06-0013, Rev. 2; 2008 Apr 16.
[24] Guzonas D, Qiu L, Edwards M. Results of bench-top chemical effects tests: Dominion – Surry 1 and 2, North Anna 1 and 2, Millstone 2 and 3. AECL Report No.: DOM-34325-TR-001 Rev. 0; 2008 July.
[25] Legg M. Millstone Unit 3 inputs for GSI-191 chemical effects testing. Dominion ERC No.: 25212-ER-06-0013, Rev. 1; 2007 Sep 24.
[26] Guzonas D, Qiu L. Chemical effects testing for Millstone Unit 2. AECL Report No.: MIL2-34325-401-000; 2008 March.